GROWTH AND DEVELOPMENT OF *SETARIA VIRIDIS* (POACEAE) UNDER NORMAL AND SHADED LIGHT REGIMES

By

QING LI

Bachelor of Science in Biology

Doane University

Crete, NE

2016

Submitted to the Faculty of the
Graduate College of the
Oklahoma State University
in partial fulfillment of
the requirements for
the Degree of
MASTER OF SCIENCE
May, 2019

GROWTH AND DEVELOPMENT OF *SETARIA VIRIDIS* (POACEAE) UNDER NORMAL AND SHADED LIGHT REGIMES

Thesis Approved:

Dr. Andrew Doust

Thesis Adviser

Dr. Ming Yang

Dr. Gopal Kakani

Mr. Chris Wood

ACKNOWLEDGEMENTS

I would first like to express the deepest appreciation to my major advisor, Professor Andrew Doust, who possesses a great passion for conducting scientific research, and is always able to come up with a lot of brilliant ideas and express unique viewpoints. He tries to spread his passion for scientific research to every student or even anyone around him, which makes people want to join his lab. Without his guidance and help, this thesis would not have been possible.

I would like to thank my committee member, Mr. Chris Wood, who is good at advising, troubleshooting, and repairing modern biological instruments, and provided help with technical issues and lab management. I have gained an immense amount of help from him in designing and building the light sources and camera system for the imaging station. Without his help, this thesis would not have gone smoothly and successfully.

I would also like to thank my other two committee members, Professor Ming Yang from Plant Biology, Ecology and Evolution Department, and Professor Gopal Kakani from Plant and Soil Science Department at Oklahoma State University. They both provided a lot of constructive insights and suggestions, and their own professional expertise, which greatly assisted this thesis.

In addition, a thank you to Professor Tessa Durham Brooks of Doane University, who guided me to complete an images analysis workshop held by them. Without the basic understanding and fundamental knowledge of imaging processing, the image analysis part of this thesis would not have been possible. I also thank Jiayuan Shi of Megvii Technology LLC, who gave me a lot of help in troubleshooting the image analysis process in this thesis by using her computational background.

Financial support was provided by the National Science Foundation.

Name: QING LI

Date of Degree: MAY, 2019

Title of Study: GROWTH AND DEVELOPMENT OF *SETARIA VIRIDIS* (POACEAE) UNDER NORMAL AND SHADED LIGHT REGIMES

Major Field: Plant Biology

Abstract: Plants rely on photosynthesis to gain energy for growth, yet most plants are found with other plants, and therefore need to deal with varying degrees of shading. Shading by plants affects both the spectrum (especially red (R) to far-red (FR) ratio) and the amount of photosynthetically active radiation (PAR, 400-700 nm). The effect of shade (shade tolerance/ shade avoidance syndrome) has been well studied in the dicot species *Arabidopsis thaliana*, but relatively little in grasses. In addition, few studies have investigated the developmental trajectory of plants under different shading treatments. The goal of this study is to understand the effect of light quality and quantity on shade responses in the C_4 grass, *Setaria viridis*. To achieve this, plants were grown under combinations of high or low light intensity, paired with high or low R:FR (mimicking sunlight or shade respectively) in continuous light. Both top view and side view images were taken at 15 min intervals during the growth of the plants, with a custom-designed imaging system that used individual Raspberry Pi NOIR cameras dedicated to each plant. Custom OpenCV scripts were written to extract relevant plant trait information from the images, including blade vertex coordinates and height. Our novel approach allows us to capture the behavior of individual organs, rather than more commonly used measures that focus on overall plant shape. By flowering time, plant shading (both simulated by the reduction of R:FR and by reduced light intensity) resulted in a significant increase of height, number of tillers, and biomass of plants. Analysis during growth and development also revealed changes in leaf orientation and increased variation in leaf position and leaf movement in plants grown under low R:FR. We found that the third leaf length and leaf growth rate was primarily influenced by light intensity, but that most other traits were influenced by either light quality or the interaction between quality and intensity.

TABLE OF CONTENTS

Chapter Page

Chapter Page

LIST OF TABLES

Table Page

LIST OF FIGURES

Figure Page

CHAPTER I

INTRODUCTION

SETARIA, A MODERN MODEL ORGANISM

In biological research, model organisms always play a crucial role in scientific discoveries, which can then be used to generalize a model that is widely applicable to other organisms. A well-known model organism is *Arabidopsis thaliana*, studies of which have contributed greatly to the knowledge of plants. For example, the discovery of the ABC model of floral development was regarded as a milestone in plant developmental biology. However, although *Arabidopsis* has been an extremely useful model for over 40 years, it cannot be regarded as the only model in plant biology. Angiosperms are a diverse group of land plants so that many traits of them are only found in particular lineages (Xianmin Diao, 2014). In particular, the C_4 photosynthetic cycle, which is used in many plant species such as species belonging to Poaceae family, are not able to be conducted in C_3 plants, as represented by *Arabidopsis*. Therefore, it is necessary to use a C4 plant as a model to investigate the phenomenon of C4 photosynthesis.

Two species in the genus of Setaria, *Setaria italica* (foxtail millet) and its wild ancestor *Setaria viridis* (green millet) are new model organisms for both monocots and C_4 plants, which have several desirable traits that are similar to those of *Arabidopsis*, such as a small stature, a small genome size, and a short life cycle. They are particularly useful also due to plentiful genomic information and being a wild-domestic pair (Xianmin Diao, 2014).

These two species are closely related to economically important crops such as maize, sorghum and switchgrass (Li & Brutnell, 2011). Phylogenetic relationships between species is one of the reference factors in choosing a model organism, because a closer relationship should indicate more similarities between two species (Doust et al., 2009).

On the one hand, Setaria is considered as a potential experimental crop model not only because it is closely related to other worldwide major crops, but the genus includes both crop and weed species (Rominger, 1962). For example, *Setaria italica* serves as a significant human crop in northern China, where it is well-known as a nourishing food source. In this case, as an experimental crop model, shading is a problem that it needs to deal with, because it requires relatively high light intensities for optimum growth but is often found in crowded prairie or crop ecosystems. On the other hand, Setaria is a good lab model due to its various intrinsic properties such as short stature, which makes it quite easy to accommodate them even in a limited space as the lab. One of the benefits of conducting experiments in the lab is that the growing conditions can easily be artificially manipulated. For example, growing plants under continuous light doesn't simulate natural growing environments, but it is a useful topic for breeders to investigate. Because it has been demonstrated that the generation cycle is shortened for some species under continuous light, this could be a huge benefit for breeders (Sysoeva et al., 2010). Conducting an experiment under continuous light in Setaria will be interesting and may benefit breeders.

MOST PLANTS HAVE TO COMPETE WITH OTHER PLANTS FOR LIGHT

Plants rely on photosynthesis to gain energy for growth, yet most plants compete with other plants for light. Light is one of the main resource components plants need for growth; plants compete for different resources including light when they grow in close proximity (H. Smith & Whitelam, 1997). Therefore, the reduction of light intensity due to overcrowding or shading in agricultural and natural settings forces plants to adapt. Due to the differences in habitats, plants

have two different strategies to deal with shading, avoidance and tolerance (Gommers et al., 2013). Shade avoidance is an approach used by plants that are found in open habitats where plants have similar heights, and involves changes in phenotype to reduce the quantity of shading in the future (Jorge J Casal, 2012; Gommers et al., 2013). It is a complex phenomenon that can involve three dimensions; vertical, horizontal and temporal. How many or which specific dimensions get involved are determined by the architecture and structure of different species. The most well-known adaptation in the vertical dimension is the elongation of the stem; in the horizontal dimension it would be the leaf reorientation; in the temporal dimension, it is early flowering, or the seed remaining dormant. Shade tolerance is a specific adaption to life in the shade, when growing out of the shade is impossible, as happens in forest understories (Gommers et al., 2013). The typical shade tolerant plants usually suppress the expression of shade avoidance syndrome symptoms (Gommers et al., 2013). For a specific example, they show a lack of stem or petiole elongation under shade environment, which differs from the shade avoidance plants (Gommers et al., 2013). Compared to shade avoidance, there are few studies that investigate the molecular pathway of shade tolerance.

SHADE AVOIDANCE

It has been suggested that the shade avoidance response evolved along with shading, when plants first colonized land in the Devonian period (S. Mathews, 2006). The term "shade avoidance" was proposed at least 40 years ago, but it is hard to find the first-time people started using it (H. Smith & Whitelam, 1997). Shade avoidance can be defined as a response to light signal change due to neighbor plants by adjustments in phenotype and function, to reduce the current and future degree of shading (J. J. Casal, 2012). It is well established that both the spectrum, especially red (R) to far-red (FR) ratio, and the amount of photosynthetically active radiation (PAR, 400-700 nm) change underneath a leaf canopy. The review paper of Casal (2012) presents this clearly, as Figure 1 shows that FR light (730 nm) is poorly absorbed by green foliage compared to R light

(680 nm), which leads to a relatively low R:FR ratio in the shaded environment. The R:FR of sunlight is about 1.18 on a clear day, while it decreases to 0.3 - 0.4 beneath the canopy (V. Deregibus et al., 1985). This change in quality of light is the main cause of the shade avoidance behavior, which has been confirmed in several experiments conducted using artificial light with uniform PAR but varying R:FR ratio, where plants such as soybean and *Chenopodium album* showed shade avoidance responses (Kasperbauer, 1987; D. Morgan & Smith, 1978). Furthermore, the R to FR ratio has been considered as a reliable signal of shading as it is hardly affected by other environmental factors (H. Smith, 1995).

Figure 1. Differences between sunlight and shade light (J. J. Casal, 2012).

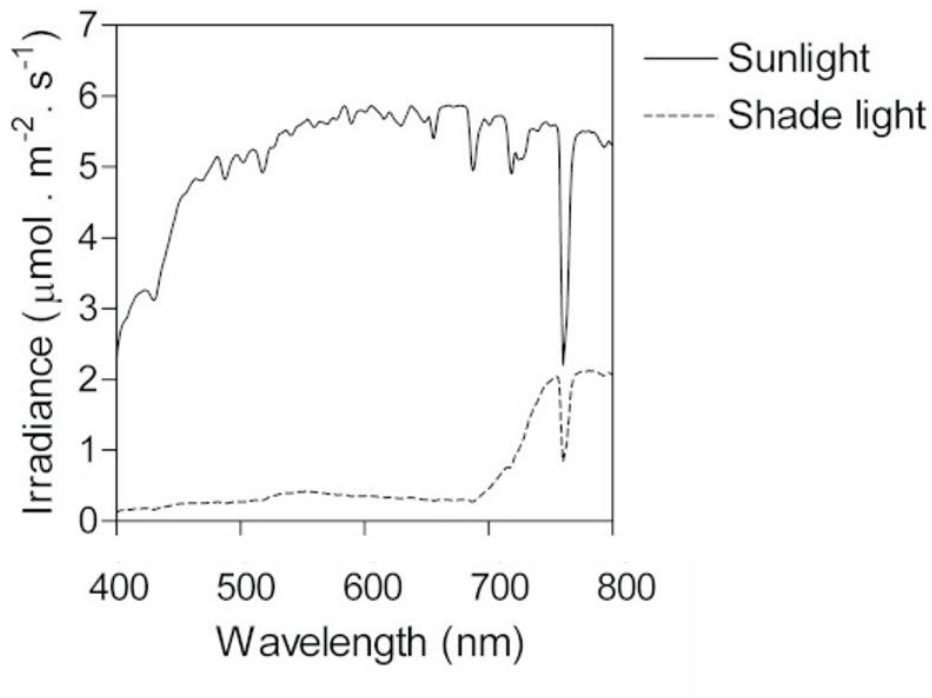

Shade avoidance syndrome

A lot of initial studies in shade avoidance were conducted in dicot models, particularly in *Arabidopsis thaliana*. Shade avoidance responses are found at all developmental stages in the life cycle of *Arabidopsis*, including repression of germination, promotion of stem elongation at the seedling stage, decrease in branching, promotion of leaf hyponasty at the rosette stage and acceleration of flowering at the flowering stage (J. J. Casal, 2012; Pedmale et al., 2010).

Compared to the dicot model *Arabidopsis*, other species, especially monocots, have been studied less, but general findings agree with findings in *Arabidopsis*. Major shade avoidance traits include stem and petiole elongation, tiller reduction, organ reorientation and early flowering; as observed in both natural and simulated conditions (J. Casal et al., 1986; Halliday et al., 1994; Maddonni et al., 2002; H. Smith & Whitelam, 1997). These traits include both growth and development of plants. By growth we mean the extension or expansion of the plant, as in size, height and biomass. More specifically, the stem and petiole elongation, and organ reorientation all can be categorized as growth traits. Development is the process by which structures originate as a plant grows, which includes the tiller production, and the transition to flowering. Different species have their own major obvious responses to shade. For example, eudicots tend to show an increase in length of stems and petioles while forage grasses tend to decrease the number of tillers (V. Deregibus et al., 1985; V. A. Deregibus et al., 1983; H. Smith, 1982). In addition, some crops display a major leaf reorientation effect, such as maize (Maddonni et al., 2002). However, the general trend of phenotypic change and the mechanistic basis are very similar in all studied species, the purpose of which is to reduce current and future degree of shading.

Most people assume that phenotypic plasticity is adaptive to a heterogeneous environment (J. Schmitt et al., 2003). However, this assumption is too arbitrary and needs to be verified in various situations. Theoretically, for phenotypic plasticity to be adaptive, the phenotypes induced

by a particular changed environment must have more fitness than the alternative phenotypes (J Schmitt, 1997). As for the shade avoidance scenario specifically, phenotypes such as stem elongation or leaf reorientation induced by a low R:FR ratio and/or low light intensity should have higher fitness in a dense planting (J Schmitt, 1997). On one hand, the stem elongation caused by low R:FR ratio enables plants to get more light in a competitive environment; on the other hand, being tall induces a higher possibility for the plant to be damaged by wind, which can bring negative effects to plants in the absence of competition (J Schmitt, 1997). Different populations growing in different habitats may have different capabilities for shade avoidance responses, which may have different adaptive values. The research conducted on *Impatiens capensis* demonstrates the adaptive differences among different species or even the same species in different habitats (Donohue et al., 2000). The genotype from an open area displayed more responses to low R:FR ratio than the genotype from a woodland environment.

Although responses to shading have been studied from many perspectives with different plant species, there have been no studies in the literature which creates a complete profile recording these responses in real-time, especially in C_4 grasses. Lack of such knowledge is an important problem, because creating a complete phenotypic profile of a plant's response to shade helps us better define the nature of shade avoidance or tolerance in these species.

Molecular mechanisms of shade avoidance

The phytochromes, a family of photoreceptors, have been identified as having the most important role in perceiving changes in light conditions in the environment and in initiating responses to shading (H. Smith & Holmes, 1977). They exist in two interconvertible forms, the biologically inactive Pr form and the biologically active Pfr form. Pr absorbs light at the peak of 660nm (R) and converts to the Pfr form, while Pfr absorbs light at the peak of 730nm (FR) and relaxes to the Pr form. A dynamic photoequilibium, i.e., the R:FR ratio, is established under any given light

condition (H. Smith & Holmes, 1977). The phytochrome genes can be classified into two major lineages in angiosperms, based on phylogenetic analyses (S. Mathews, 2006). One includes PHYB and PHYB-related genes, and the other contains PHYA and PHYC (S. Mathews, 2006). Different species have different numbers of phytochrome members. For example, *Arabidopsis* has phyA, phyB, phyC, phyD, and phyE in which phyD and phyE are phyB-related photoreceptors, while only three members including phyA, phyB, and phyC are in rice (S Mathews & Sharrock, 1997; Reed et al., 1993). Among all members in the phytochrome family, phyB and phyA play the most crucial role in majority of shade avoidance responses (J. J. Casal, 2012). Compared to phyB, phyA is quite insensitive to R:FR ratio change, and its activity is hardly affected until the R:FR reaches below 0.3 (H. Smith et al., 1997). However, phyA has ability to detect the irradiance changes caused by shade (Sellaro et al., 2010). In addition, phyA works against phyB by constraining hypocotyl elongation under low R:FR condition and mediates some shade avoidance responses in de-etiolating seedlings (Johnson et al., 1994; Quail, 1994). Besides the change of R:FR ratio, blue light and UV light also change under shade, which involves some other photoreceptors, such as cryptochromes, phototropins, and UVR8 (J. J. Casal, 2012).

The signaling network that controls shade avoidance syndrome is well established. The molecular regulation of the shade-avoidance syndrome has been well summarized by Gommers et al. (2013) as shown in Figure 2. Phytochrome existing in an active Pfr form in the nucleus normally binds or degrades some portion of PHYTOCHROME-INTERACTING FACTORS (PIFs), while the rest of the undegraded PIFs are bound by DELLA proteins (Djakovic-Petrovic et al., 2007). The first identified PIF was PIF3 and was followed by other closely related PIFs (Ni et al., 1998, 1999). Under the canopy, due to the reduced R:FR ratio, Pfr converts to inactive Pr form, which leads to the disassociation with PIFs and exiting from the nucleus. In other words, the inactivation of phyB results in an increase of nuclear PIFs. Consequently, PIFs bind to

target promoters and regulate gene expression related to elongation growth such as auxin synthesis genes to promote shade avoidance response (L. Li et al., 2012). The genes first proposed to be regulated by altered R:FR ratio were a group of HD-Zip class II subfamily transcription factors including ATHB2 and ATHB4 (Carabelli et al., 1993). Meanwhile, GA-mediated DELLA degradation also increases under the low R:FR condition, which relieves the inhibition of PIF activity, and further leads to the increase of nuclear PIFs (Djakovic-Petrovic et al., 2007). Hormones besides auxin and gibberellins have also been found to play a role in response to shading, including brassinosteroids, cytokinins, and ethylene (J. J. Casal, 2012).

Figure 2. Simplified overview of molecular regulation behind shade avoidance responses

Arrows indicate positive regulation, blunt arrows indicate negative regulation (Gommers et al., 2013).

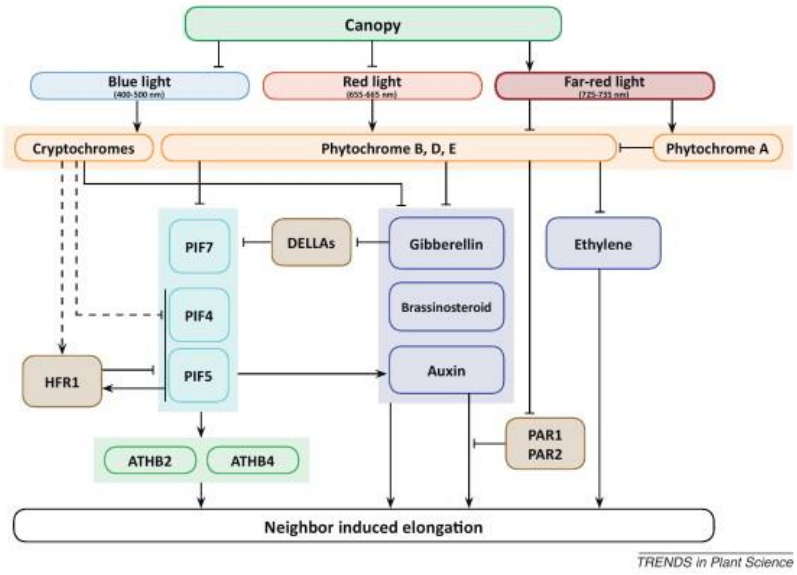

DIFFERENT STAGES OF SHADING

Plants detect their neighbor's existence before getting physically blocked by the neighboring vegetation, by sensing changes in light quality (Ballaré et al., 1987). Besides full sunlight and extreme shade, there are other illumination conditions a plant may experience in a canopy (Jorge J Casal, 2012). A plant can receive full vertical and horizontal propagating light plus additional FR light in a sparse canopy from its neighbors compared to a fully isolated plant because of the light reflection from the leaves of its neighbors (Figure 3B). Another stage between the one just stated and the deep shade light condition is where the vertical organs of plant are shaded by its neighbors. In this case, there is some reduction of the horizontal propagating light intensity and the R to FR ratio is still lower than the isolated plant (Figure 3C). Both horizontal and vertical propagating PAR is reduced in a dense canopy when neighboring plants cause physical interference (Figure 3D). Shade avoidance changes are caused by the reduction of the R to FR ratio (H. Smith & Holmes, 1977). Plants are expected to show some shade avoidance phenotypes from the detection of neighbors from the second stage (Figure 3B) they experience in the growing canopy; they receive increased FR light and approximately constant red light.

Figure 3. Four stages a plant may experience in a growing canopy (adapted from J. J. Casal, 2012).

A) Plant fully isolated from the surroundings. B) Plant receiving reflected FR light from neighbors but not shaded by neighbor plants. C) Vertical organs of plant shaded by leaves of neighbor plants. D) Plant fully shaded by surroundings.

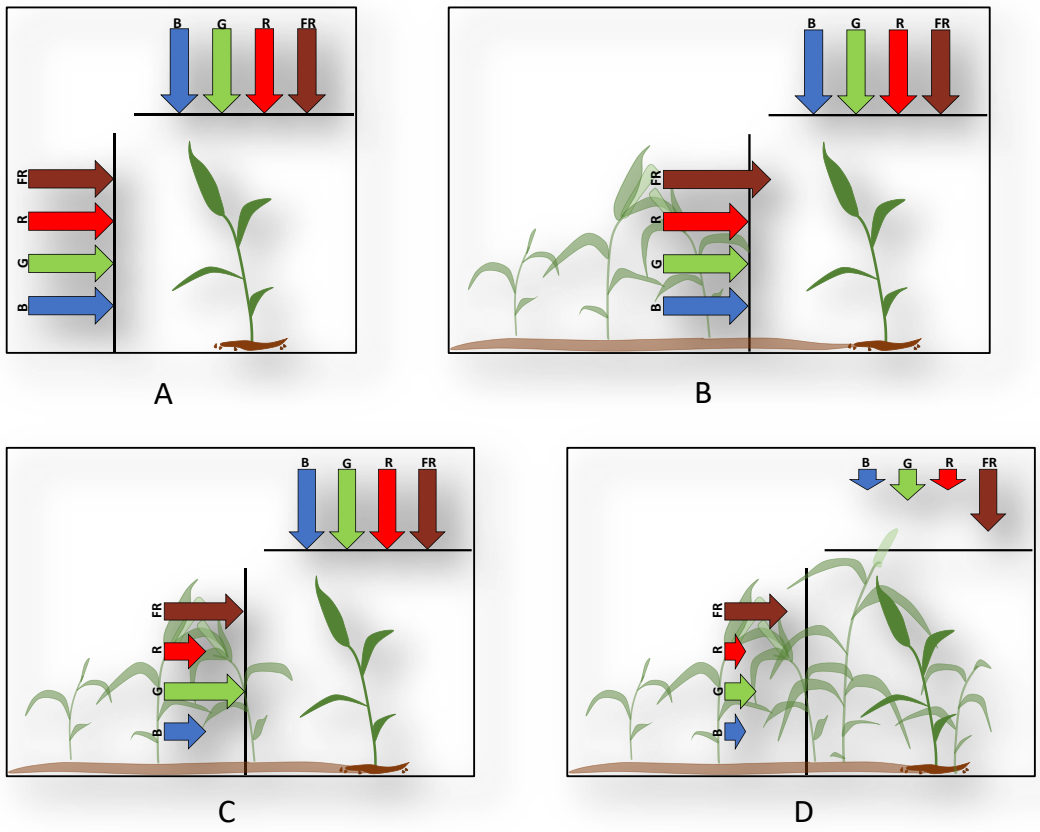

NECESSITY OF USING HIGH-TEMPORAL RESOLUTION AND HIGH-THROUGHPUT PHENOTYPING TECHNIQUE

Collecting phenotype data manually is time consuming and prone to error (Gehan & Kellogg, 2017), and the measurements are often only taken at one or a few time points. This is known as the "phenotyping bottleneck" (Furbank & Tester, 2011). To solve this problem, researchers have developed automated and lower-cost methods for data collection and analysis, collectively known as "high-throughput phenotyping" (Gehan & Kellogg, 2017). High-throughput phenotyping is defined as a technology that can automatically collect much more data in specific images per day than a manual approach. The Raspberry Pi camera is a convenient tool that researchers can use for high throughput phenotyping data collection due to it being inexpensive and portable (Mutka & Bart, 2014). After obtaining a collection of images, a simple analysis pipeline can quickly be applied to the image data. PlantCV was developed by researchers specifically for plants, and makes data analysis relatively simple (Jorge J Casal, 2012; Gehan & Kellogg, 2017). PlantCV enables automated pipelines to be constructed, which reduce a lot of user input requirements compared to other conventional image processing software such as ImageJ (Easlon & Bloom, 2014).

Temporal resolution refers to the ability of distinguishing two events on time scale. For example, you expect two packages delivered to your house while you are not home and arrival time difference between those two packages is half an hour. If you have a camera taking photos every ten minutes in front of your house, you will know which package come first. However, if your camera taking photos every hour, you could not figure out the order. This example demonstrates the importance of high-temporal resolution photographing on distinguishing developmental sequences. In the field of Botany, measurements generally taken at one or several time points during the whole experiment will result in lots of details and processes missing between two

snapshots. With the development of this technology, high temporal resolution phenotyping appears achievable, and especially necessary for exploring the growth and development of plants.

CHAPTER II

THE EFFECT OF SHADING ON TIME TO FLOWERING AND ARCHITECTURE AT FLOWERING TIME OF *SETARIA VIRIDIS*

INTRODUCTION

There are several ways to test a plant's response to shading, either by using other plants to provide shading or by simulating aspects of shade lighting conditions. The most common method of simulation is to reduce the ratio of R:FR, while keep light intensity the same, in order to separate the effects of resource availability (amount of light available for photosynthesis) from any effect of shading as a morphogenetic signal to the shaded plant. In addition, the change of light intensity under shade has been considered a less reliable signal than the change in R:FR (H. Smith & Whitelam, 1997). To achieve low R:FR condition under shade, researchers add additional FR to normal light conditions. Experiments using this method in *Arabidopsis thaliana* detected an acceleration of flowering time and a reduction of leaf number under low R:FR (Halliday et al., 1994). In other species such as *Chenopodium album*, seedlings grown with additional FR (low R:FR) are taller than the control group (D. C. Morgan & Smith, 1976). In grasses, an increase in R:FR for *Paspalum dilatatum* and *Sporobolus indicus* increased tiller number and total dry weight (V. Deregibus et al., 1985), while in *Lolium multiflorum*, a decrease in R:FR led to a reduction of tillers, acceleration of flowering, and elongation of leaf sheath and blades (J. Casal,et al., 1985).

Besides the addition of FR or R, another method to simulate shading signals is using a pulse

of far-red light at the end of the photoperiod (EOD-FR). The principle of this method is to change the status of phytochromes that persist during the subsequent night period (J. J. Casal, 2012). The EOD-FR treatment resulted in increased growth of petioles and accelerated flowering time in *Arabidopsis* (Devlin et al., 1996), and increased mesocotyl and first leaf sheath length in maize (Dubois et al., 2010). People rarely simulated shade light signals by changing the light intensity alone, as the reduction of R:FR perceived by phytochrome is considered to be an indispensable component of shade avoidance syndromes (H. Smith & Whitelam, 1997).

Some experiments investigated the influence of light intensity on plants by grouping plants in different densities, and found the number of tillers reduced and dry weight per unit leaf area decreased under low PAR in *Lolium spp*. (Mitchell, 1953). However, the R:FR ratio status in this type of experiment changes between the groups, which makes it hard to conclude which components caused the phenotypes. In addition, plants are competing not only for light but also for other resources, such as water and nutrients.

Relatively few studies have examined light quantity and light quality as independent variables, especially in grasses. One study attempted this in sorghum by measuring growth under different light regimes and separating Photosynthetic Photon Flux Density (PPFD) and R:FR components (Finlayson et al., 2007). Using red and far-red LED light sources, they used ratios of 0.50 and 2808 R:FR for low R:FR and high R:FR, respectively; with 20 $\mu mol \cdot m^{-2} \cdot s^{-1}$ and 140 $\mu mol \cdot m^{-2} \cdot s^{-1}$ for low and high light intensity. These intensities and ratios are far removed from normal sun and shade conditions, with normal sun intensities of 1600-2000 $\mu mol \cdot m^{-2} \cdot s^{-1}$ and R:FR of ~1.2 and shade intensities in the region of ~200 $\mu mol \cdot m^{-2} \cdot s^{-1}$ and R:FR of ~0.3-0.5 (L. Milenkovic et al., 2012). They found that increasing FR under either high or low light results in slower elongation of the leaves, which is different from the classic shade avoidance syndromes reported above. However, the level of red light used is extreme, and the possibility exists that it was physiologically damaging to the plant. Leaf elongation was measured at 5 days old over a 10

hour span, and the authors use the elongation rate of blade:sheath as an index of shade avoidance response (Finlayson et al., 2007). The increase of FR caused a reduction of the blade:sheath elongation rate, which is consistent with previous findings in rice (J. Casal et al., 1996) but opposite to that found by Dubois (2010). Reduction of PPFD also resulted in the same result, the reduction of the blade:sheath elongation rate.

Since the differing roles of light quantity (intensity) and quality (R:FR ratio) in shade avoidance syndromes are not clear, we decided to conduct an experiment to dissect the effect of light intensity and light quality on plant growth in a balanced experimental design. Based on previous studies, we hypothesize that Setaria plants would likely flower faster under low R:FR, and have reduced tiller numbers and longer stems under both low R:FR and low light intensity.

METHODS

Plant materials and growing conditions

Setaria viridis (A10) were grown in 7.6 cm diameter round black pots with Sun Gro Horticulture standardized soil under artificial lights with a 24-h day length. Water was applied when necessary. Plants were grown under either higher (designated 'normal') or lower (designated 'low') light intensities, paired with R:FR ratios mimicking sun ('normal' R:FR) or shade ('low' R:FR), depending on which trial they were in. The normal light level treatment was much less than full sun, but is designated as normal because it produces consistent and rapid growth and flowering, as determined in previous trials (Doust et al. 2017). The low light level treatment was approximately one-third of the normal light level treatment. R:FR ratios for the normal level treatment were somewhat higher than that found in full sunlight (~1.5 as opposed to ~1.2), and the low level R:FR treatment ratio was similar to plant shade (~0.3). Detailed information of light intensity and R:FR of each trial is listed below.

Light source construction

The light source used in this experiment was constructed based on three 43cm*122cm*8cm regular T5 regular fluorescent light racks, each originally with six bulbs. To increase light intensity, twelve more fluorescent light bulbs were installed on these three racks. One bar with red and far-red LEDs was fixed in the middle of each rack. In summary, the light source is made up by 30 T5 HO fluorescent light bulbs, three LED bars mounted with four red (660 nm) LEDs and four far-red (740 nm) LEDs on each. The light intensity produced by red and far-red LEDs can be tuned by an Arduino controller, in order to adjust the R:FR ratio. More details of the LED bar can be found in Figure 4. The overall appearance of the lighting structure can be seen in Figure 5.

Figure 4. The illustration of the LED bar circuit.

Colored curve lines represent wires. Yellow square rectangles contain a detailed explanation of the function of each part.

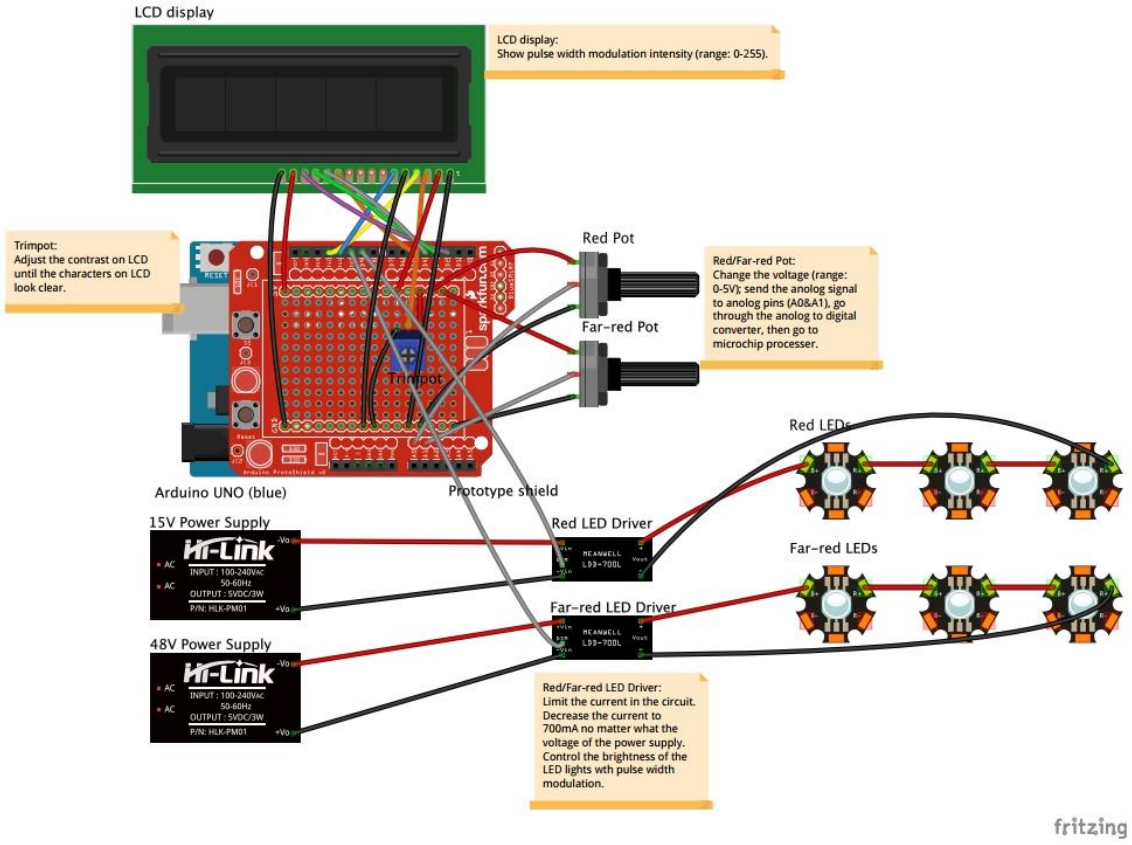

Figure 5. Overall appearance of lighting structure (Top view).

Red circle represents red LED; white circle represents FR LED; grey bar represents fluorescence light bulb. Green circles are where the pots were placed.

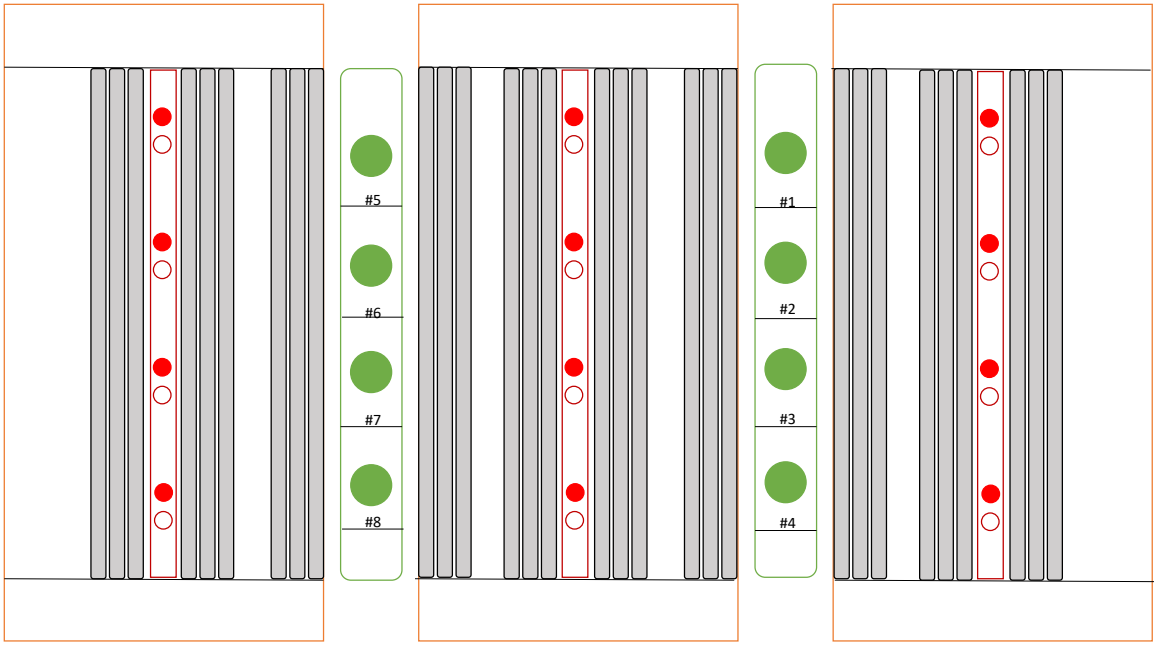

Growth trial: normal light intensity with normal R:FR

Eight individual Setaria plants were grown under the constructed light banks, as shown in Figure 5. The total light intensity and R:FR ratio at each plant position was in the range of 300-380 $\mu mol \cdot m^{-2} \cdot s^{-1}$, and 0.28-0.43, respectively, depending on which plant position. More specific data on each position can be found in Table 1. Plants were germinated in an off-site common environment, with light intensity of 440 $\mu mol \cdot m^{-2} \cdot s^{-1}$ and R:FR of 3.18, before being transferred to the experimental set-up at the two-leaf stage. Plants were then imaged in the experimental set-up for two weeks, before being removed to a relatively similar amount of light and R:FR environment according to the specific trial until flowering. To avoid reflected light affecting plant responses in both the pre and post common growth conditions and in the experimental set-up, cloth cylindroid barriers were provided as borders for each plant. Cylindroids were made from regular poster board and covered with black shade cloth, to make the background consistent, and to facilitate image analysis. The long axis of the cylindroid was 55cm, the short axis was 30cm, and the height was 20cm. These dimensions were chosen so as to separate each plant, while at the same time not blocking too much light for each plant. The shade cloth was also tested to make sure that it did not reflect any wavelength of light differentially. Each set of light intensity and R:FR treatments was repeated twice with eight replicate plants in each. Images of the experimental setup can be found in Appendix 1.

Growth trial: normal light intensity with low R:FR

To simulate shading artificially, instead of using real plants, far-red light bars were used to provide a more controllable light environment. Two far-red light bars were mounted on the top, to reduce the entire R:FR ratio. FR light intensity was adjusted to make a R:FR of 0.3-0.4. The change in total light intensity occasioned by the introduction of the FR LEDs was negligibly small. All other settings were the same as in the normal light intensity/normal R:FR trial, except

that R:FR ratio was decreased as stated above. More detailed information on each spot can be found in Table 2. Even though there is variation of light intensity and R:FR among spots, we found no correlation between R:FR or light intensity with the measured traits.

Growth trial: low light intensity with low R:FR

In order to create a low intensity trial, twenty fluorescent light bulbs were removed. The entire light intensity was decreased to about one third of the original, averaging 110 $\mu mol \cdot m^{-2} \cdot s^{-1}$. The R:FR ratio remained as 0.3-0.4. All other settings were the same as the normal light intensity/normal R:FR trial, except that both R:FR ratio and total light intensity were decreased as stated above. More detailed information on each spot can be found in Table 3.

Growth trial: low light intensity with normal R:FR

In order to create a low intensity trial with normal R:FR, the additional far-red light bars were taken off. All other settings were the same as with the normal light intensity/normal R:FR trial except that total light intensity was decreased as stated above. More detailed information on each spot can be found in Table 4.

Table 1. Light intensity and R:FR ratio on each position of growth trail—normal light intensity/normal R:FR.

	Pos.1	Pos.2	Pos.3	Pos.4	Pos.5	Pos.6	Pos.7	Pos.8
Light intensity ($\mu mol \cdot m^{-2} \cdot s^{-1}$)	300	357	370	330	312	380	320	315
R:FR ratio	1.55	1.48	1.48	1.58	1.61	1.48	1.41	1.41

Table 2. Light intensity and R:FR ratio on each position of growth trail—normal light intensity/low R:FR.

	Pos.1	Pos.2	Pos.3	Pos.4	Pos.5	Pos.6	Pos.7	Pos.8
Light intensity ($\mu mol \cdot m^{-2} \cdot s^{-1}$)	300	357	370	330	312	380	320	315
R:FR ratio	0.28	0.30	0.39	0.33	0.43	0.41	0.38	0.39

Table 3. Light intensity and R:FR ratio on each position of growth trail—low light intensity/low R:FR.

	Pos.1	Pos.2	Pos.3	Pos.4	Pos.5	Pos.6	Pos.7	Pos.8
Light intensity ($\mu mol \cdot m^{-2} \cdot s^{-1}$)	103	120	128	107	101	104	110	113
R:FR ratio	0.30	0.34	0.32	0.30	0.29	0.30	0.34	0.32

Table 4. Light intensity and R:FR ratio on each position of growth trail—low light intensity/normal R:FR.

	Pos.1	Pos.2	Pos.3	Pos.4	Pos.5	Pos.6	Pos.7	Pos.8
Light intensity ($\mu mol \cdot m^{-2} \cdot s^{-1}$)	113	133	132	113	108	137	134	122
R:FR ratio	1.43	1.41	1.54	1.71	1.54	1.54	1.43	1.42

Phenotypic measurements

The number of days from planting to the first appearance of the inflorescence on the main culm (days to heading) were recorded as the measurement of time to flowering. Total number of leaves, total number of tillers, shoot height to the uppermost ligule, and length and width of the newest expanded blade were recorded on the heading day. Inflorescence length was recorded when the inflorescence was fully expanded. Shoots were then collected and dried in order to measure shoot dry biomass.

Statistical analysis

The mean and confidence limits for all eight traits were graphed, and pair-wise correlations calculated between each pair of traits. All traits were analyzed with a two-way analysis of variance (ANOVA), to test the effects of light intensity and light quality and their interaction. Partial eta squared values were calculated by $\frac{SS_{Effect}}{SS_{Effect} + SS_{Error}}$ (SS: Sum of Squares) to estimate the proportion of variance explained by each factor or their interaction for each collected phenotypic measurement. In all above analyses, the criterion for significance level was set at $P < 0.05$. All statistical analyses were performed using R version 3.5.3.

RESULTS

Multiple traits were measured at flowering time, including height, number of leaves, days to flower, number of tillers, youngest expanded leaf length and width, inflorescence length, and dry shoot biomass (Figure 6). The pattern of variation varied amongst the traits, but the plants in the low light intensity/decreased R:FR ratio ($L_lL_{R:FR}$) treatment stood out by exhibiting the highest number of leaves, the longest and widest leaves, the greatest height, the longest inflorescence, the occasional presence of tillers, the highest biomass, and the longest time to flowering. Taken as a whole, plants in the low light intensity/normal R:FR ratio treatment ($L_lN_{R:FR}$), were at the

opposite end of the spectrum, being short, with fewer and narrower leaves, shorter inflorescence, no tillers, and low biomass. Differences were few between the two normal light intensity treatments, although the treatment with the low R:FR ratio had taller plants than the normal R:FR ratio.

Correlations between traits

To estimate the relationships between traits, pair-wise correlation analyses were performed for each treatment (Table 5). There was a strong positive correlation between leaf length and leaf width, as well as between number of leaves, height, and biomass. The relationships between days to flower and inflorescence length and days to flower and leaf length were significantly negative in all treatments but $L_IL_{R:FR}$. Biomass positively correlated with leaf length and leaf width in $L_IL_{R:FR.}$ Interestingly, the relationship between days to flower and the other seven traits was either non-significant or showed a significant negative correlation.

Table 5. Correlations between traits in each of four treatments at flowering time.

The value of the Pearson correlation coefficient (r) and the significance level as stars are shown (each significance level is associated to a symbol: p-value < 0.001("***"), 0.001 < p-value < 0.01 ("**"), p-0.01 < value < 0.05 ("*"). Non-significant values were not shown in the graph. $L_IL_{R:FR}$: Low light intensity with Low R:FR; $L_IN_{R:FR}$: Low light intensity with Normal R:FR; $N_IL_{R:FR}$: Normal light intensity with Low R:FR; $N_IN_{R:FR}$: Normal light intensity with Normal R:FR.

Traits	Days to flower	Number of leaves	Height	Number of tillers	Leaf length	Leaf width	Inflorescence length	Dry biomass
Days to flower	$L_IL_{R:FR}$		-0.58*					
	$L_IN_{R:FR}$	-0.51*	-0.81***		-0.85***	-0.87***	-0.89***	-0.79***
	$N_IL_{R:FR}$				-0.59*		-0.71**	
	$N_IN_{R:FR}$		-0.55*	-0.59*		-0.65**	-0.55*	-0.65**
Number of leaves		$L_IL_{R:FR}$						
		$L_IN_{R:FR}$	0.80***		0.77***	0.68**	0.68**	0.80***
		$N_IL_{R:FR}$	0.80***					0.66**
		$N_IN_{R:FR}$	0.60*					0.59*
Height			$L_IL_{R:FR}$				0.55*	
			$L_IN_{R:FR}$		0.92***	0.89***	0.96***	0.9***
			$N_IL_{R:FR}$					0.80***
			$N_IN_{R:FR}$			0.58*		0.81***
Number of tillers				$L_IL_{R:FR}$				
				$L_IN_{R:FR}$				
				$N_IL_{R:FR}$				
				$N_IN_{R:FR}$			0.62**	0.68**
Leaf length					$L_IL_{R:FR}$	0.78***		0.53*
					$L_IN_{R:FR}$	0.91***	0.91***	0.93***

		$N_IL_{R:FR}$	0.69**	0.74**	0.70**
		$N_IN_{R:FR}$	0.59*		
Leaf width			$L_IL_{R:FR}$		0.53*
			$L_IN_{R:FR}$	0.92***	0.94***
			$N_IL_{R:FR}$		
			$N_IN_{R:FR}$		0.58*
Inflorescence length				$L_IL_{R:FR}$	
				$L_IN_{R:FR}$	0.87***
				$N_IL_{R:FR}$	0.75***
				$N_IN_{R:FR}$	0.57*

The effect of light intensity, light quality and their interaction on certain phenotypic traits

The effect of light intensity, light quality and their interaction on each of the eight collected traits at flowering time was analyzed with two-way ANOVAs. Partial eta squared values and the significance level for the two-way ANOVA for each trait are presented in Table 6. More detailed results from the two-way ANOVAs can be found in Appendix 2.

Several patterns of significance were observed in the data. Days to flowering was significant for light intensity and quality but not their interaction, with only a low proportion of the variance accounted for by these factors (low partial eta squared values). All other traits showed significant interactions between intensity and quality. Three traits, leaf number, height, and inflorescence length, were significant for light quality and the interaction of quality and intensity, but not for intensity alone. Leaf length showed an opposite pattern, being significant for light intensity and the interaction of quality and intensity, but not quality alone. Tiller number showed significance only for the interaction between quality and intensity. Finally, leaf width and biomass were significant for both quality and intensity and their interaction.

Figure 6. Flowering-time measurements of Setaria under normal or low light intensity with normal or low R:FR.

Circle with the bar represents the mean and 95% confidence interval. $L_IL_{R:FR}$: Low light intensity with Low R:FR; $L_IN_{R:FR}$: Low light intensity with Normal R:FR; $N_IL_{R:FR}$: Normal light intensity with Low R:FR; $N_IN_{R:FR}$: Normal light intensity with Normal R:FR

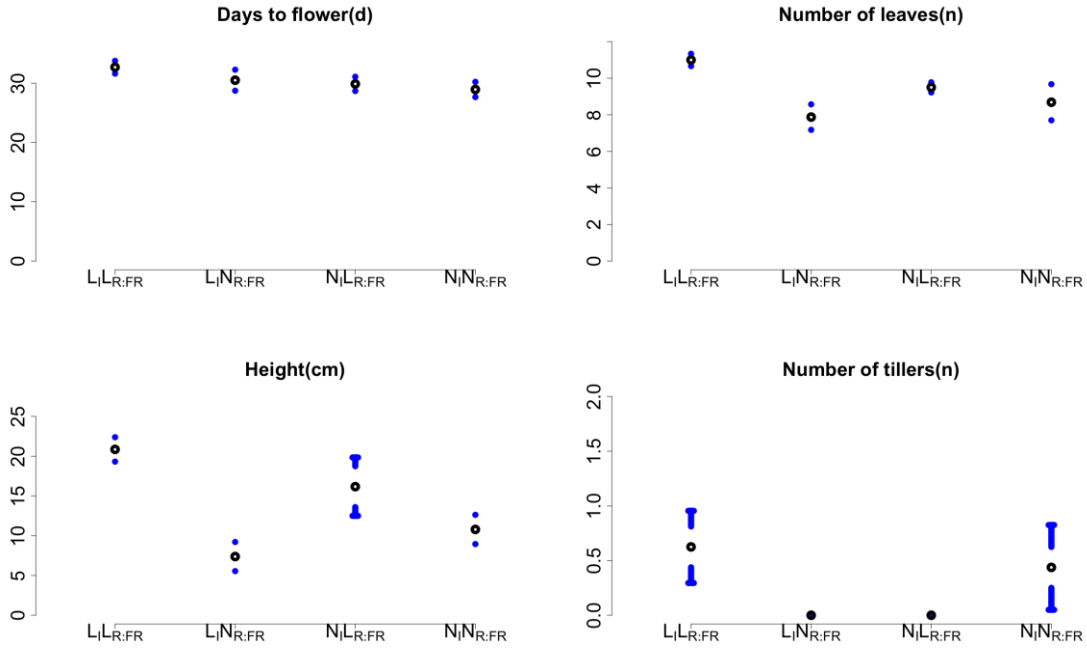

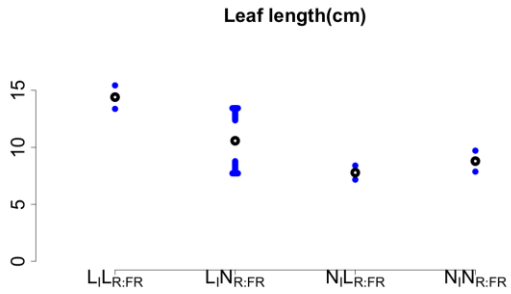
Leaf length(cm)
0
5
10
15
LILR:FR
LILN:FR
NILR:FR
NILN:FR

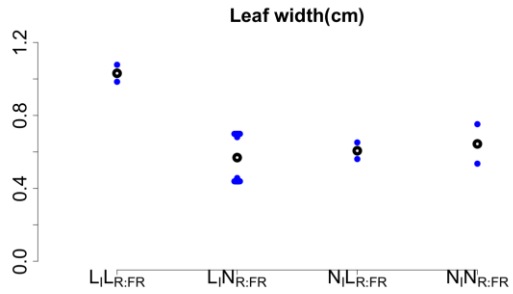
Leaf width(cm)
0.0
0.4
0.8
1.2
LILR:FR
LILN:FR
NILR:FR
NILN:FR

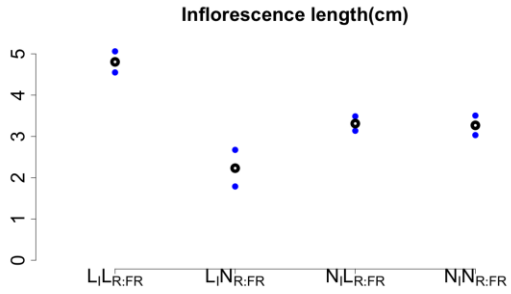
Inflorescence length(cm)
0
1
2
3
4
5
LILR:FR
LILN:FR
NILR:FR
NILN:FR

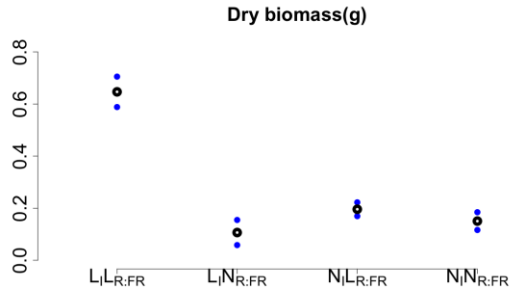
Dry biomass(g)
0.0
0.2
0.4
0.6
0.8
LILR:FR
LILN:FR
NILR:FR
NILN:FR

Table 6. Effect size and significance level for the two-way ANOVA of the eight phenotypic measurements at flowering time. The larger the partial eta-squared value the greater effect of that factor. P-value < 0.05 labeled as *; P-value < 0.01 labeled as **; P-value < 0.001 labeled as ***. All partial eta-squared values that were significant are highlighted in bold.

Trait	Source factor	Partial Eta Squared (Significant level)
Days to flower	Light intensity	**0.16****
	Light quality	**0.09***
	Light intensity × light quality	0.016
Number of leaves	Light intensity	0.021
	Light quality	**0.42*****
	Light intensity × light quality	**0.20*****
Height	Light intensity	0.0054
	Light quality	**0.54*****
	Light intensity × light quality	**0.18*****
Number of tillers	Light intensity	0.010
	Light quality	0.010
	Light intensity × light quality	**0.25*****
Leaf length	Light intensity	**0.34*****
	Light quality	0.055
	Light intensity × light quality	**0.14****
Leaf width	Light intensity	**0.22*****
	Light quality	**0.29*****
	Light intensity × light quality	**0.37*****
Inflorescence length	Light intensity	0.043
	Light quality	**0.60*****
	Light intensity × light quality	**0.58*****
Dry biomass	Light intensity	**0.62*****
	Light quality	**0.77*****
	Light intensity × light quality	**0.71*****

DISCUSSION

Summary of the plant's phenotypes under different light conditions

The plants under $L_IL_{R:FR}$ treatment showed the most differences in architecture from the other three treatments. They grew about 1.5 to 3 times taller, developed an inflorescence that was about 1.5 to 3 times longer, leaves that were wider and 1.5 to 2 times longer than the plants growing under the other three treatments. Compared to the differences between $L_IL_{R:FR}$ and other three treatments, the differences among the other three treatments are relatively small. The overall shape of the plants under $L_lN_{R:FR}$, $N_IL_{R:FR}$ and $N_IN_{R:FR}$ groups are very similar, but varied in size. Plants under $L_lN_{R:FR}$ had the smallest size, with the smallest stature, shortest inflorescence, fewest and narrowest leaves. Plants under $N_IL_{R:FR}$ are slightly greater in size than plants under $N_IN_{R:FR}$. The promotion of shoot elongation in $L_IL_{R:FR}$ was expected, since it is part of the shade avoidance syndrome as traditionally defined. However, the other two main classic shade avoidance syndrome symptoms, reduced tillering and accelerated flowering time, were not found in this experiment. Instead, not much variation showed in tiller number and flowering time between four treatments, which suggests that Setaria also showed some degrees of shade tolerance characteristics.

Light intensity, light quality, and their interaction all play roles in the plant's response to shading

Although light intensity, light quality, and their interaction showed different effects on different traits, they all played roles in the plant's response to shading to some extent, regardless of the effect size, and the number of traits they played roles in. It is noteworthy that light quality showed a significant effect on six out of eight phenotypic traits we collected, compared to four for light intensity. This suggests that light quality, probably mediated through phytochromes, plays an indispensable role in the plant's response to shading, as has been found in previous

studies. However, our finding disagrees with previous reports that the reduction of light intensity is not a reliable signal under shade (H. Smith & Whitelam, 1997).

Dry shoot biomass dramatically increased under $L_IL_{R:FR}$

The dry shoot biomass showed a significant greater value in $L_IL_{R:FR}$ treatment than the other three treatments, which is not an expected result. There are two possible explanations of this phenomenon. As mentioned above, Setaria displayed some degrees of shade tolerance characteristics in this experiment including flowering time and tiller numbers, therefore, one of the explanation is that the increase of dry shoot biomass at flowering time under natural shading environment could be regarded as another performance of shade tolerance feature. Another one is regarding as the biomass allocation. A shifting of the biomass allocation from roots to aboveground structures is a common shade responses in grasses (Dias-Filho, 2000). Therefore, this increase of dry shoot biomass could be a result of biomass allocation shifting under shade environment. This could be tested by including the dry root biomass as well in the future experiment.

Size of leaves becomes a main factor of determining biomass under $L_IL_{R:FR}$

Under all conditions but $L_IL_{R:FR}$, the dry shoot biomass is positively correlated with number of leaves, height, and inflorescence length. In addition, biomass is also positively correlated with the number of tillers in $N_IN_{R:FR}$. However, biomass is only positively correlated with leaf length and leaf width in $L_IL_{R:FR}$, suggesting that the major growth in these plants is in the leaves.

The novelty of our experimental design

It is not completely surprising that some of our results differ from previous findings, because our experimental design was explicitly created to test differences between both light quantity and quality separately, unlike most previously published studies. The most similar experimental

design to ours, which also separated the light intensity and R:FR elements, is the one of Finlayson et al., 2007. They used 20 $\mu mol \cdot m^{-2} \cdot s^{-1}$ and 140 $\mu mol \cdot m^{-2} \cdot s^{-1}$ for low and high light intensity, and 0.50 and 2808 for low and high R:FR. These intensities and R:FR ratios are extremely different than that of sunlight (the R:FR of sunlight is ~1.18). Their lighting values are the result of using custom red and far-red diode arrays. The extremely low light intensities are unlikely to induce normal growth in a C4 grass like sorghum or Setaria. In contrast, the light intensity and R:FR used in our experiment are greater, with approximately 300 and 100 $\mu mol \cdot m^{-2} \cdot s^{-1}$ for normal and low intensities, and ~1.5 and ~0.3 R:FR ratios for high and low R:FR. Our normal light treatment is clearly much less than full sunlight, but previous experiments in our lab have shown that Setaria plants grow well at this light intensity (Doust et al. 2017). Even though the normal R:FR we used (~1.5) does not perfectly match sunlight, it is not only much closer, but can also mimic the environment in some greenhouses which contain more red light for production purposes. In addition, almost all previous experimental setups were confounded by the spectrum changing between low and normal light intensity groups, or by allowing interactions between neighboring plants (Bailey et al., 2001; Mitchell, 1953). In contrast, our experimental set-up maintained the same spectrum under different light intensities, and the same light intensity under different spectrums. We also removed other potential confounding variables, including plant to plant reflection of FR light, by surrounding individual plants with a black elliptical cylinder. Our results therefore are explicitly limited to the interaction of individual plants with simulated shading, and will allow us to further explore the effects of directional shading. The novel, inexpensive, and precise data collection and analysis pipeline will also facilitate new explorations of how the developmental trajectory of plants is affected by biotic and abiotic interactions, as discussed in the next chapter.

CHAPTER III

THE EFFECT OF SHADING ON GROWTH AND DEVELOPMENT OF *SETARIA VIRIDIS* PLANTS

INTRODUCTION

Plants are inextricably shaped by the environment in which they grow. Unlike animals, they cannot move to avoid environmental stress. Thus, of the two main mechanisms that organisms utilize to deal with environmental stress, evasion and coping, animals prefer to evade via their movement and behavior, while plants necessarily have to cope with the stress where they are (Huey et al., 2002). There is no doubt that animals can relieve stress by moving from an unfavorable locality to one that is more favorable, for example, moving from direct sun in the heat of the day to the shade of a rock, or hunting at cooler times of the day (Huey et al., 2002). Plants don't possess this ability, as the body of a plant is rooted in one place throughout its life. However, plants can adapt by differential growth to the conditions they find themselves in (Huey et al., 2002). Even though plants are unable to move to a more agreeable place like animals do, they can avoid or reduce the stress by changing their morphology. Morphological changes include but are not limited to growing taller, branching more or less, branching on one side but not the other, and leaf or stem reorientation. These reactions can also be categorized as response mechanisms, although these are not as obvious as in animals. Therefore, the phenotype of a plant is intimately related to its environment, and show a wide range of architecture differences caused

by the environment, a phenomenon which is known as plasticity. While it is known that plants utilize differential growth to respond to environmental stimuli, in most cases the manner in which such growth occurs is inferred from the resultant morphology, rather than observed during growth itself. In addition, the respective contributions of development and environment to the resulting morphology are unclear, because it is relatively difficult to provide a plant with a constant environment. The aim of this chapter is to examine the developmental variation of growth, and how the quantity and quality of light affect growth forms of a member of the Poaceae family, *Setaria viridis*.

METHODS

Plant materials and growing conditions

The data in this study represent the developmental data from the growth trials described in chapter II, except images were collected every 15 minutes on a custom-designed imaging system, from the two-leaf stage to approximately the five leaf stage.

Image collection

In each black cylindroid chamber, a slanted mirror was placed beside each plant to capture the side view in addition to the top view of the plant. Plants were oriented parallel to the fluorescent lights and to the mirrors. Eight NoIR (no infrared light filter present) Raspberry Pi cameras were mounted above each plant on the rack to record the dynamic growth of the plant from both side and top views every fifteen minutes throughout the experiment. A digitally switchable power strip (PowerSwitch Tail) was used to provide a safe way for the Raspberry Pi to control the fluorescent and LED lights. Eight infrared lights were mounted evenly on the rack to cover the entire rack with infrared light, which enabled the cameras to capture images of the seedlings when the fluorescent and LED lights were off. Infrared lights were covered by small pieces of

regular white printer paper to help diffuse the light. A Python script was run to control the PowerSwitch Tail which was connected to all light sources in this experiment. The idea of the script is to turn off all the light sources for 10 seconds before the NoIR Raspberry Pi cameras take photos, for the purpose of simplifying the image processing procedures later. In this case, all photos were taken every fifteen minutes under infrared lights during 24 hours in the course of 14 days.

96 images were created from each Raspberry Pi camera per day and they were stored in a folder on the desktop on Raspberry Pi. Each image used 618.3 Kb space on the Raspberry Pi. The image resolution is 72 dpi.

Image processing and image information acquisition

Over the course of 6 to 15 days (depending on how fast the plant grew out of the boundary of the mirror), both side view and top view image sets were run through several custom OpenCV scripts to do image processing such as thresholding, masking, extracting relevant plant trait information such as identifying the blade vertex coordinates, and height, and to perform the image processing operations. Some major steps of image processing are shown in Figure 7. Information was exported as a csv file, for further data processing analyses. After extracting the vertex coordinates of the first four leaves from both top and side view images for each replicate plant, three-dimensional coordinates were obtained by combining the two sets of information. The x, y coordinates were obtained from the top view image, and the z coordinate information was gained from the side view image. This is illustrated in Figure 8.

Measurement of height, number of flowers, and distance between successive leaves at 9 days from germination

To compare the growing status of a plant at a particular uniform stage among different groups, the ninth day after germination was chosen and the first image of that day was selected for each

of the 64 plants (16 replicates per treatment, 4 treatments in total). Leaf number and x, y coordinates of several points including the starting point, all ligules, and the third leaf tip were saved in a csv file. An illustration of the extracted traits can be found in Figure 9. Most information could be derived from the csv file containing the data of all different time points, which was stated above. A few points were not identified by the program successfully, and ImageJ analysis software was used to compensate for it. Twenty images were randomly chosen to verify the consistency of the result from ImageJ and the custom OpenCV script. The absolute differences between the results of the two programs for each coordinate were smaller than 2 pixels. The distance between the first ("2" in Figure 9A) and second ("3" in Figure 9A) ligule was calculated as the difference between the first and second leaves; the distance between the second and the third ("4" in Figure 9A) ligule was calculated as the difference between the second and third leaves; and the distance between the third ligule and the third leaf tip ("5" in Figure 9A) was calculated and used as an estimation of the third leaf blade length. The distance between the starting point ("1" in Figure 9A) and the topmost ligule was calculated as the height.

Measurement of third leaf growth rate

To compare the growth rate of the same leaf among different groups, two images were selected from each of the 64 plants. The first one is the image at the stage at which the third leaf just appears, and the second one is 10 hours after the first one. The third leaf tip information was saved in a csv file of both images, and the distance between two points divided by 10 hours was used as the estimated growth rate of that plant. The length of the fully expanded third leaf at the initial of 5-leaf stage was also measured. The strategy is same as the measurements stated above, except the top view was used this time, due to the mirror size limitation. The x and y coordinate of third leaf tip at 5-leaf stage and the starting point was recorded, for calculating the distance between these two points (Figure 9B).

Measurement of leaf erectness

Leaf openness was used to describe the degree of the third leaf erectness. The side view images of the plants at 11 DAG were used to achieve this purpose. More specifically, the culm of the plant was used as the vertical axis. Another line was drawn between the tip and the ligule of the third leaf on the side view image by ImageJ. The angle between this line with the vertical axis was measured by ImageJ and the data was recorded into a csv file. This method of measuring the leaf erectness was adapted from Yoshida et.al., 1969.

Measurement of degree of leaf growth deviation from perfect 180˚ phyllotaxy

To quantify the degree of the randomness of the plant growth form at a relatively late vegetative stage, the eleventh day after germination was chosen and the first image of that day was selected from each of the 64 plants (16 replicates per treatment, 4 treatments in total). A minimum rotated bounding rectangle was fitted for each plant on the image, and the width of the rectangle was recorded. The width of the rectangle is a representative of the deviation of the leaf growth from perfect 180˚ phyllotaxy. Figure 11 contains two comparable examples. Figure 11A has a greater rectangle width than Figure 11B, which corresponds to the leaves in Figure 11A growing at angles that deviate more from 180˚ than Figure 11B. This was calculated using a custom OpenCV script. The input of the script are the images at 11 DAG for all 64 plants, and the output is a csv file containing the information of image id, center of the rectangle, height and width of the rectangle, and the rotated degree of the rectangle.

Statistical analyses

As with the results at flowering time, data of three measurements extracted from different images including number of leaves, height and the length of the internode, third leaf length, and the third leaf growth rate were analyzed with a two-way ANOVA to test the effects of light intensity, light quality, and their interaction on the traits. Partial eta squared values were calculated by

$\frac{SS_{Effect}}{SS_{Effect} + SS_{Error}}$ (SS: Sum of Squares) to estimate the proportion of variance explained by each factor or their interaction for each collected phenotypic measurement. The criterion for significance level in the analysis was set at $P < 0.05$. Statistical analyses were performed using R version 3.5.3.

Figure 7. Major steps of image processing.

A) Original image taken by the NoIR Raspberry Pi camera. B) Mask image of top view. C) Mask image of side view after 90° degree rotate. D) Top view mask image with all identified blade vertexes. Each blue dot represents one blade vertex. E) Side view mask image with all identified blade vertices and the points of the junction of leaf and leafstalk (position of ligule). Each blue dot represents a blade vertex, and each green dot represents a ligule. F) Top view mask image with correctly labeled blade vertex. Red, blue, green, aquamarine represent first, second, third, fourth blade vertex respectively. G) Side view mask image with correctly labeled blade vertex and uppermost ligule. Color code of blade vertex is same with the top view image. Purple represents the uppermost ligule.

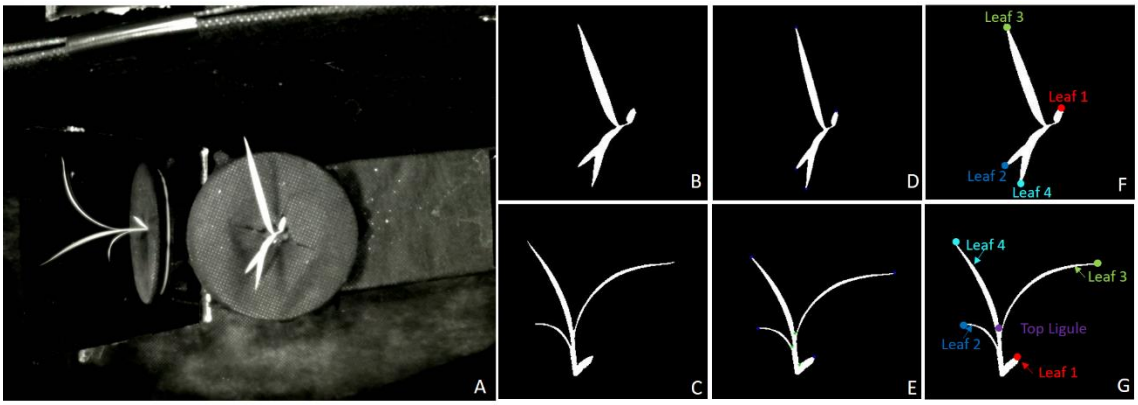

Figure 8. Illustration of three-dimensional model construction.

Two overlapped time shots of side view (left) and top view (right) of a plant with one image semi-transparent. $A(x_1, y_1)$ of the top view and $A(y_1, z_1)$ of the side view are the same point (both second blade vertex) in the earlier stage. $B(x_2, y_2)$ of the top view and $B(y_2, z_2)$ of the side view are the same point (both second blade vertex) in the later stage. $C(y_0, z_0)$ is the original point of the plant. The second blade vertex of two time shots (A, earlier time shot; B, later time shot) are plotted in the three-dimensional plot.

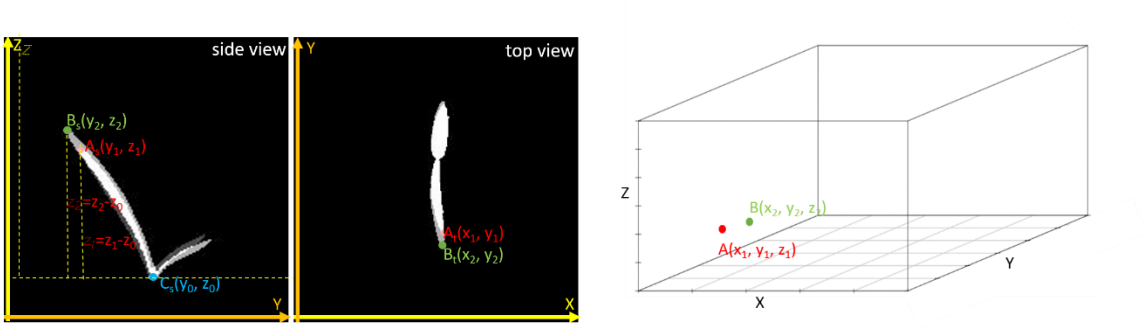

Figure 9. Illustration of information extracted from the image.

A) Image at 9 DAG stage with labeled points. 1-5 red dot represents the starting point, first ligule, second ligule, third ligule and the third leaf tip, respectively. B) Image at initial 5-leaf stage with labeled points. Two Red dots represent the starting point and the third leaf tip, respectively. The length of the red line is an estimation of the third leaf length.

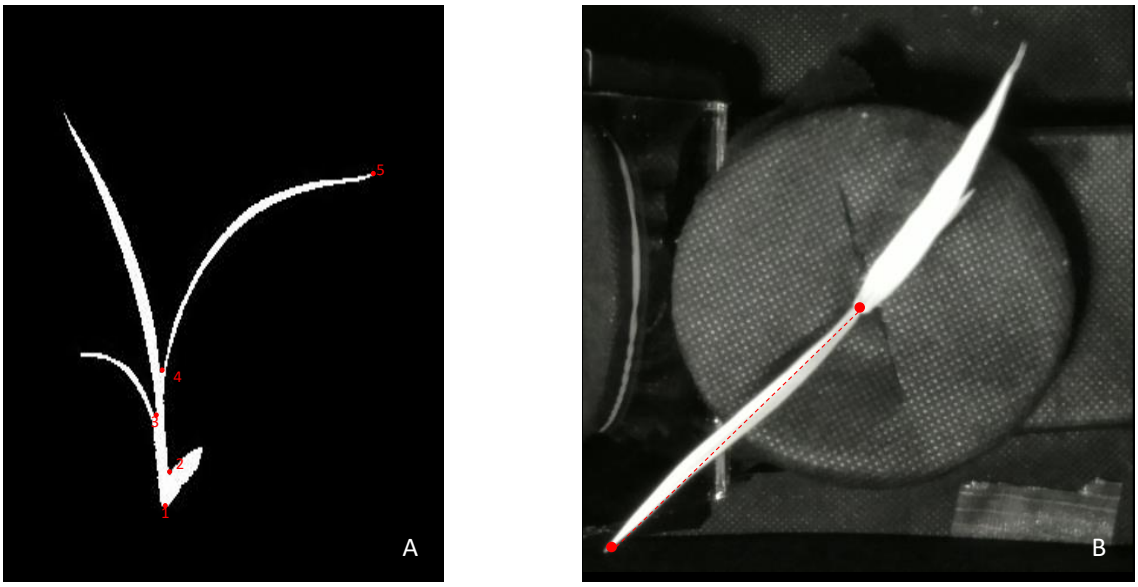

Figure 10. Illustration of the acquisition of the leaf erectness degree information on a side view image.

Two yellow lines represent the vertical axis, and the line between the tip and the ligule of the third leaf tip.

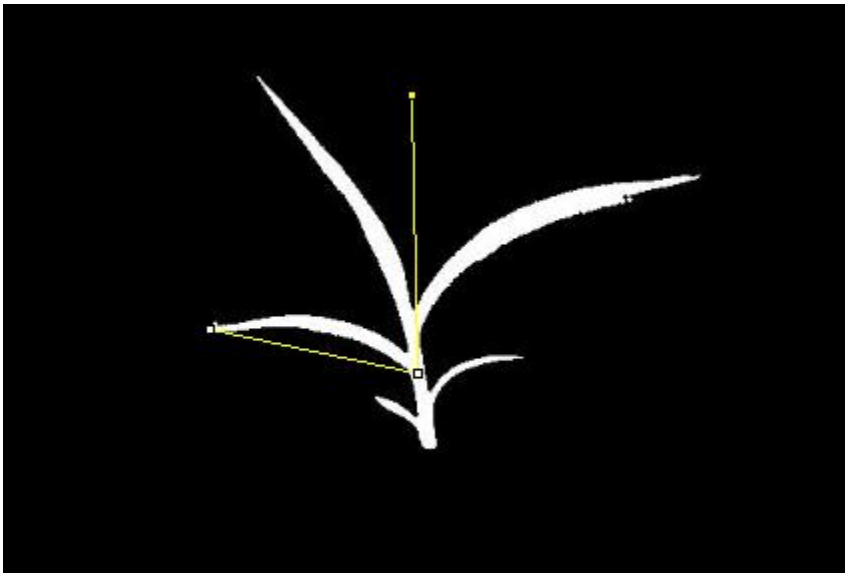

Figure 11. Examples of two plants have different fitted rectangle width corresponding to different randomness of the growth form.

The white rectangle is generated by a custom OpenCV script, which is drawn with minimum areas**.**

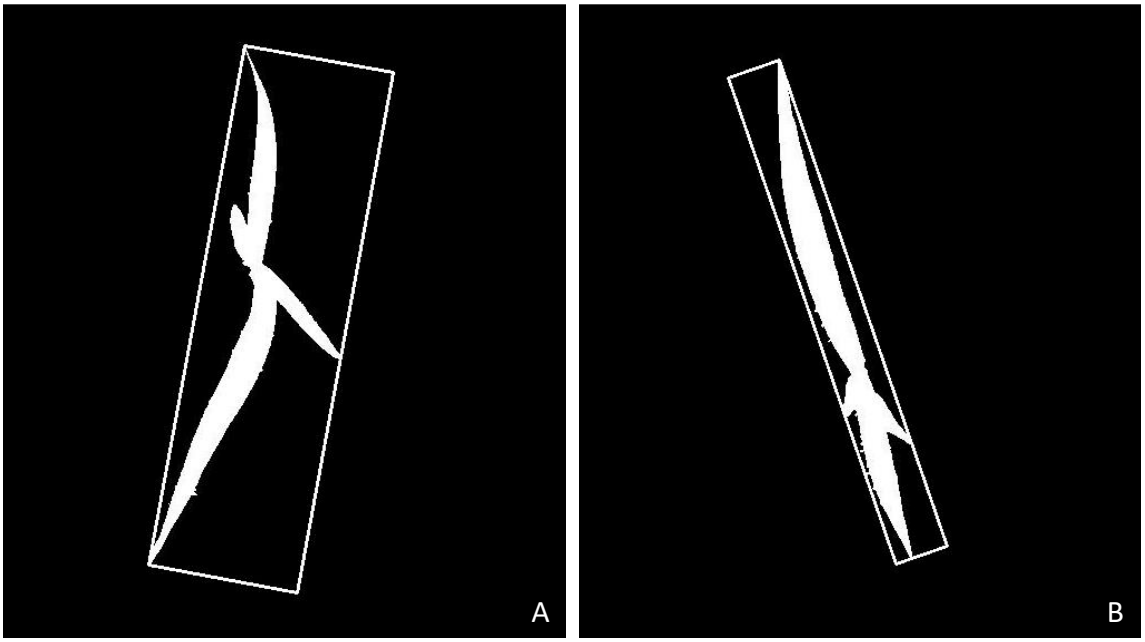

RESULTS

Multiple traits were extracted from the collected developmental images, including height at 9 DAG, distance between successive leaves at 9 DAG, number of leaves at 9 DAG, length of the third leaf, and the growth rate of the third leaf (Figure 12). First, to summarize the traits acquired from the images at 9 DAG, the plots of height and distance between successive leaves share a similar pattern, where the plants in the low light intensity/low R:FR ($L_lL_{R:FR}$) treatment stood out by displaying a much greater stature and a longer distance between successive leaves than the other three treatments. The plot of the number of leaves presents a different pattern, where plants growing under low R:FR had more leaves than plants under normal R:FR with the same light intensity. For the plots of the length and growth rate of the third leaf, plants under low light intensity showed a slower growth rate but a longer leaf than the plants under normal light intensity when they had same R:FR ratio.

The effect of light intensity, light quality and their interaction on collected phenotypic traits

The effect of light intensity, light quality, and their interaction on each of the traits in the vegetative stage was analyzed with two-way ANOVA. Partial eta squared values and the significant level for two-way ANOVA for each trait are presented in Table 7. More detailed results of two-way ANOVA can be found in Appendix 3.

Several patterns of significance were observed in the data. Height and the distance between successive leaves were significant for both quality and intensity and their interaction. Number of leaves was significant for light intensity and quality but not their interaction. The length and growth rate of the third leaf were significant only for intensity alone. The other two traits showed in this table will be mentioned in the following text.

Leaf growth was affected by the change in light intensity in opposite directions

Based on the two-way ANOVA analysis, we conclude that both the third leaf length and the growth rate of the third leaf were only affected by the change of light intensity, but not light quality or their interaction. A better understanding of the direction of the effect needs to be determined from analysis of the image plots (Figure 12). The growth rate of the third leaf was decreased by the reduction of the light intensity under both low and normal R:FR. Interestingly, the plot of the third leaf length actually showed an opposite trend from the plot of the third leaf growth rate. Specifically, the leaf length under low light intensity ended up with a longer leaf than the plants under normal light intensity with the same R:FR (Figure 12). It is worth noting that plants under the same light intensity shared very similar values in both plots, which means the plants developed similar leaf length and had similar leaf growth rates when they received the same light intensity but different R:FR ratios. This result suggests that both leaf length and leaf growth rate were affected by the change of light intensity, but in opposite directions.

Figure 12. Several measurements of Setaria at early vegetative stage under normal and low light intensity with normal or low R:FR.

Circle with the bar represents the mean and 95% confidence interval. $L_IL_{R:FR}$: Low light intensity with Low R:FR; $L_IN_{R:FR}$: Low light intensity with Normal R:FR; $N_IL_{R:FR}$: Normal light intensity with Low R:FR; $N_IN_{R:FR}$: Normal light intensity with Normal R:FR

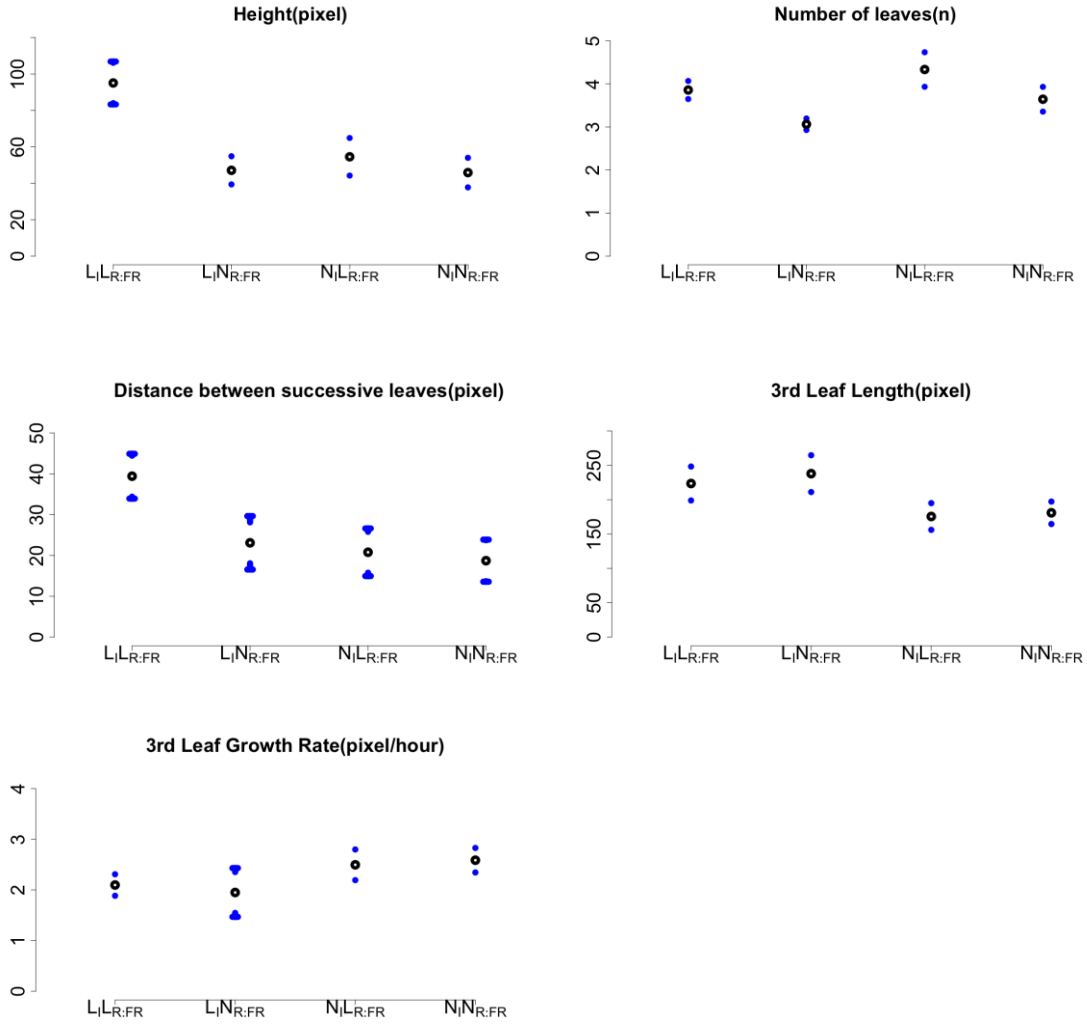

Table 7. Effect and significance level for the two-way ANOVA of seven traits extracted from images at vegetative stage. P-value < 0.05 labeled as *; P-value < 0.01 labeled as **; P-value < 0.001 labeled as ***. All partial eta-squared values that were significant are highlighted in bold.

Trait	Source factor	Partial Eta Squared (Significance level)
Height	Light intensity	**0.28*** **
	Light quality	**0.43*** **
	Light intensity × light quality	**0.26*** **
Distance between successive leaves	Light intensity	**0.24*** **
	Light quality	**0.17** **
	Light intensity × light quality	**0.11***
Number of leaves	Light intensity	**0.24*** **
	Light quality	**0.38*** **
	Light intensity × light quality	0.0030
Third leaf length	Light intensity	**0.31*** **
	Light quality	0.016
	Light intensity × light quality	0.0033
Third leaf growth rate	Light intensity	**0.16** **
	Light quality	0.00057
	Light intensity × light quality	0.0099
Δz	Light intensity	**0.35*** **
	Light quality	0.0014
	Light intensity × light quality	0.030
Rectangle width	Light intensity	**0.12** **
	Light quality	**0.30*** **
	Light intensity × light quality	**0.11** **

Leaves are more erect under low light intensity

Three-dimensional coordinates of each leaf vertex through time were plotted in a graph during the interval between the initiation of the two-leaf stage to the end of the four-leaf stage. The plots of leaf trajectory movement suggest that the direction and angle of the blade behaved differently under different light conditions. In the two normal light intensity treatments, the third leaf of all the replicate plants grew upwards and then gradually bent downwards under the weight of the leaf (Figure 13A&B). However, the action of bending downwards almost disappeared in the two low light intensity treatments, where leaves only showed upward growth (Figure 13C&D).

To further quantify our observation, we used the side view image of the plants at 11 DAG. We drew a line between the leaf tip and ligule of the third leaf, and use the culm itself as the vertical axis. The angle between this two line was measured. This value represents the degree to which the leaf opens. The mean and confidence interval plot confirms the observations that plants grown under low light intensity had a significant smaller leaf openness than the plants growing under normal light intensity (Figure 14), which suggests that plants grow more erect under low light intensity. A two-way ANOVA was conducted on this trait, and it showed that only light intensity had a significant effect.

Plants grow more randomly under natural shaded environment

Besides the angle leaf discussed above, the plots also showed the consistency of the replicate plants' growth in different light conditions. To judge the consistency in the plot, we mainly observed the shape of the leaf growth trajectory of each replicate plant. It is noted that plants in $L_IL_{R:FR}$ had less obvious consistency than the other three groups (Figure 13). Especially during the later stages of plant growth, the leaf development of different plants performed differently and started to grow in different directions.

To look at the plant growth on a large scale through the entire recorded period, all collected images from the two-leaf stage to the four or five-leaf stage were synthesized to a short video for each plant. By going through all videos of different treatments, we noticed that for plants under normal light intensity and normal R:FR the growth trajectories grew tighter than for other trials. Most of the leaves achieved their orientation pretty quickly and eventually followed a distichous (180˚) pattern. However, in other shaded environments especially the natural shaded group ($L_IL_{R:FR}$), leaf angle deviated markedly from 180°.

To further test our observation, we fitted a minimum rotated bounding rectangle for each plant on the image at 11 days after germination, and recorded the width of the rectangle. The width is a representative of the deviation in leaf growth. The mean and confidence interval plot demonstrate our observations (Figure 15) that plants under a shading environment, especially under low light intensity and low R:FR, had a significantly wider rectangle than the other three treatments, which indicates that leaf growth deviated more in that treatment versus the others.

Figure 13. Leaf 3 growth trajectories between the two-leaf and four-leaf stages under different light conditions.

A) Leaf 3 growth trajectories in ; B) Leaf 3 growth trajectories ; C) Leaf 3 growth trajectories; D) Leaf 3 growth trajectories $L_IN_{R:FR}$.

Each color represents one replicate plant in that particular treatment.

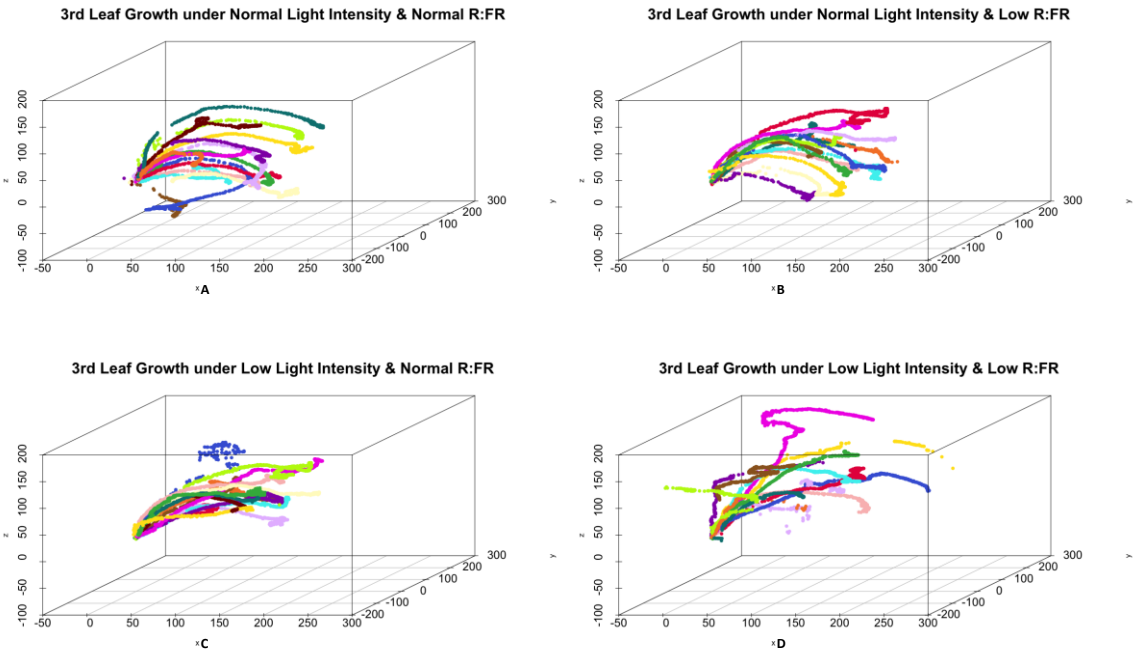

Figure 14. Measurements of the angle of the third leaf.

Circle with the bar represents the mean and 95% confidence interval. $L_IL_{R:FR}$: Low light intensity with Low R:FR; $L_IN_{R:FR}$: Low light intensity with Normal R:FR; $N_IL_{R:FR}$: Normal light intensity with Low R:FR; $N_IN_{R:FR}$: Normal light intensity with Normal R:FR

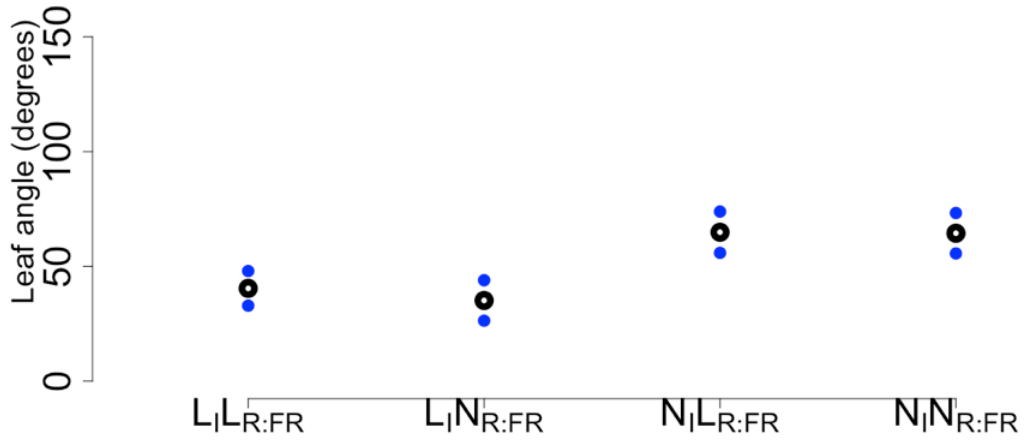

Figure 15. The width of the best-fit rectangle covering the plants from the top view under normal and low light intensity with normal or low R:FR.

Circle with the bar represents the mean and 95% confidence interval. $L_IL_{R:FR}$: Low light intensity with Low R:FR; $L_IN_{R:FR}$: Low light intensity with Normal R:FR; $N_IL_{R:FR}$: Normal light intensity with Low R:FR; $N_IN_{R:FR}$: Normal light intensity with Normal R:FR

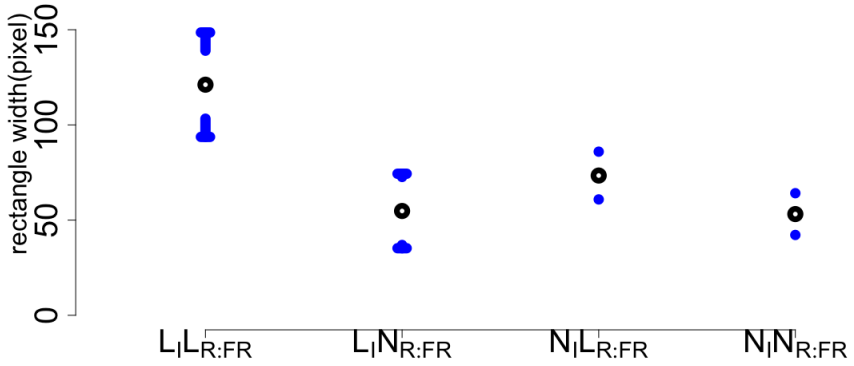

DISCUSSION

Light intensity, light quality, and their interaction all play roles in the early responses of plants to shading

As a whole, light intensity, light quality, and their interaction all played roles in the plant's early response to shading, which is similar to to our conclusions from flowering time (Chapter II). However, they showed different effects on the measurements extracted from the images during the vegetative stage.

Light is used by the plant both as fuel for photosynthesis, where intensity is particularly important, and as a signal for developmental decisions, where quality is most important. Thus, it is not surprising that light intensity had a great effect on traits such as leaf length, leaf growth rate, and the degree of leaf erectness. The decrease of the light intensity caused a slower growth rate but a longer and more erect leaf. However, the change of R:FR ratio appears to affect plant architecture, which may explain why changes in R:FR ratio have a significant effect on height, number of leaves, and the degree of leaf growth deviation from a theoretical 180˚ phyllotaxy.

Leaf length is likely to be determined by the length of the growth interval

The negative correlation between third leaf growth rate and the final third leaf length suggests that the longer leaves found in those treatments with low growth rates are the result of a longer growth period (Figure 12). Additional FR light causes a greater growth rate at the early stage, but does not necessarily lead to a longer leaf.

Setaria reacts to low R:FR at a relatively early stage

We have noticed that the trend of the plots at 9 DAG and at flowering time for the two of the same measured traits, height and number of leaves, are very similar (Figure 6 and Figure 12). The promotion of the shoot elongation in $L_lL_{R:FR}$ treatment was obvious, and it appeared again in

the height plot at flowering time. The plot of the number of leaves at 9 DAG and at flowering time showed a similar story (Figure 6 and Figure 12). The pattern of an increase in number of leaves in the low R:FR under both low and normal light intensity at 9 DAG, was also evident at the flowering stage, showing consistency between the different measurement timepoints.

Setaria shows an increase of leaf erectness (hyponasty) under shaded conditions

An increase in erectness of leaves (hyponasty) is a classic shade avoidance syndrome that is well documented in Arabidopsis. In previous studies, researchers claimed that either light quality or light quantity change would cause varying leaf inclination (Millenaar et al., 2005; Mullen, Weinig, & Hangarter, 2006). In our experiment, we observed this syndrome under the two treatments with low light intensity, but not in the other two groups with normal light intensity (Figure 14). We conjecture that the change of light intensity is the main factor triggering this phenomenon. The leaves of a plant may to have evolved a strategy of growing more erect in low light intensity in order to move closer to the source of light, such as growing out of a canopy of competing plants.

Leaves may have the ability to grow into areas of better light

We found that leaf arrangement is more variable in shaded conditions, and we conjecture that this is possibly connected to responding to a variable light environment. It is well established that roots possess the ability of growing into the potential space that can be utilized for their optimal growth (Yokawa & Baluška, 2018). Based on our analysis of the series of collected images, we speculate that shoots might show analogous movements to roots. The twisting movement of the shoot of the grass plant might be due to its growing towards a more satisfactory light environment for its development. It is likely that a slight heterogeneity was introduced into the light environment experienced by the plant by the presence of the mirror, which introduced a small difference in light conditions, including both light intensity and light quality, between the side

towards the mirror and the side opposite to the mirror. The small differences might have had greater consequences at low light intensity or low R:FR level than at high light intensity or R:FR levels, which could be a possible explanation of why we found that the leaf growth deviated more in $L_IL_{R:FR}$ versus the others. To further test this hypothesis, a better controlled heterogeneous environment could be provided in future experiments, for example, by placing a far-red light source in one direction to greatly decrease the R:FR ratio of that side. The direction of leaf growth should change if our hypothesis holds, more likely turning away from the additional far-red light source placed on that side.

CHAPTER IV

CONSTRUCTION OF A LOW-COST AND HIGH-TEMPORAL RESOLUTION IMAGING STATION

For the purpose of recording plant growth every 15 minutes, a low-cost imaging station was constructed in our lab. This imaging system allows us to analyze the collected images more easily because all images have the same light background. Detailed explanation of the imaging station construction will be found below.

MATERIALS

Fluorescent growth light panel, Model #1FD82A, Grainger International, Illinois

Fluorescent growth light bulbs, Model #F45W-T5-865, GE Lighting, Ohio

Additional light bulbs, Model #Sun Blaze 960320, Hawthorne Gardening, Washington

Far-red LED grow light bar, Model #R-22-I-1-06-N5-R, Fluence Bioengineering, Texas

PowerSwitch Tail II, Model #8016, PowerSwitchTail.com, Hawaii

Raspberry Pi 3, Model # LYSB01C6EQNNK-ELECTRNCS, CanaKit, British Columbia, Canada

NoIR camera boards with LS-2717CS CS mount lens, Product ID B0036, Arducam, New York

48-led CCTV IR lamps, Model #4331021825, Phenas, Guangdong, China

7-port Ethernet hub D-Link, Model #DUB-H7, Taiwan, China

LED Engin Far-red 740 nm LEDs with MCPCB heat sinks, Part #897-LZ440R3080000, Mouser Electronics, Inc., Texas

Red 660nm LEDs with MCPCB heat sinks, Model #HH-3WP2JR06-T, Amazon, Inc., Washington

Aluminum bars, Model #11303, The Hillman Group, Ohio

LED driver, Model #LDD-1000HW, LED Supply Company, Vermont

Metro 328 micro controller, Model #2488, Adafruit, New York

Security camera wall mount bracket, Model #0746060131147, Wasserstein Home, Hong Kong, China

Real Time Clock (RTC) board, Model #3386, Adafruit, New York

OVERALL IMAGING STATION STRUCTURE

Three 60cm*120cm*200cm growth racks were used in this experiment. One modified 43cm*122cm*8cm regular T-5 fluorescent growth light panel was hung on the top of each rack. A detailed explanation of modification is in the following. Two far-red Fluence RAY LED grow light bars were attached to the rack with metal chains in between of every two fluorescent growth light panels as an additional far-red light source, which were needed in some of the trials. The power supplies for all light sources were controlled by two DC-actuated power cords, PowerSwitch Tail II. The PowerSwitch Tails were controlled by a python script running on a Raspberry Pi 3 (RasPi) single board computer. The PowerSwitch Tails were connected to IO pins

on the main RasPi so that the on-off condition of the lights can be programmed by the RasPi python script. The script, which can be found in the Appendix, basically turns off all the lights for IR photography, and then tells the eight RasPis with NoIR cameras to take images sequentially. These two steps were repeated every fifteen minutes during 24 hours. Infra-red lights for photography was provided by eight Phenas 48-led CCTV IR lamps. They were evenly mounted on the rack, to cover the entire rack with infra-red light. They were also covered by a piece of white printer paper, to help diffuse the light. Two rows of Setaria (four plants in each row) were placed under every two light panels. Each plant was surrounded by a black cylindroid to avoid light reflection from neighboring plants. One slanted mirror was placed on the top of each tray and right beside each plant, so that the top camera is able to capture both the top and side view of the plant. Eight RasPis with eight NoIR cameras were used, each of them in charge of one plant. The NoIR camera is situated directly above the plant. Further details of installing cameras, testing cameras, focusing, and other options can be found below. The eight RasPis were hooked up to an Ethernet hub so that they are on the same local area network (LAN). All of the RasPis and the Ethernet hub were located on the top of the growth rack. One monitor, mouse, and keyboard were connected to the main RasPi on a separate table in the same room. This setup allowed easy communication with the eight RasPis via ssh and virtual network connection (VNC) protocols since all were on the same LAN.

CONSTRUCTION OF LIGHT SOURCES

Modification of regular fluorescent growth light panel

Fluorescent growth light panels with original six T-5 light bulbs were used as the main light resource for this experiment. To increase the total light intensity to reach Setaria growth requirement, three more light bulbs were added to the outer panels, and six more light bulbs were added to the inner panel. One self-contained LED bar was added to the middle of each growth

light panel. Each bar was constructed with four LED Engin Far-red 740 nm LEDs and four Red 660nm LEDs. The LEDs on MCPCB heat sinks were mounted to 2.5 mm thick aluminum bars that provided additional heat dissipation. The two types of LEDs were separately connected in series and controlled via PWM using a 700 mA led driver from LED Supply Company. The PWM controller was constructed from an Arduino based micro controller.

Additional FR light source

Fluence RAY LED grow light bars were used to complement FR light intensity provided by the self-contained LED bars. Light intensity of the Fluence RAY LED grow light bars can be adjusted by a powered dimmer. This allowed modification of the R:FR ratio.

CONSTRUCTION OF PHYSICAL PLANT GROWTH CONDITIONS

Three-inch black round pots filled with Sungro Horticulture standardized soil were used for the experiment. Round pots can be orientated based on the initial leaf orientation. Trays used for the experiment were clear but fully covered by black shade cloth. Cylindrical light barriers (cylindroids) were made with regular poster board and covered by black shade cloth, to make the background consistent, and easy to separate from the plants for image analysis in the future. The long axis of cylindroid was 55cm and the short axis was 30cm, the height of the cylindroid was 20cm. In this case, cylindroids were able to separate each plant, and at the same time did not block too much light for the plant.

CONSTRUCTION OF IMAGING SYSTEM

Construction and installation of RasPi camera holders

Eight Arducam NoIR camera boards with an LS-2717CS CS mount lens for RasPi were used to take images. The camera boards were mounted on small pieces of wood with four drilled holes,

which about the same size of the board, by screws at four corners. A connection nut was glued on the back of the wood. Security camera wall mount brackets were attached to the rack by cable zip ties. Another same size connection nut was screwed up on the bottom of camera wall mount bracket. Camera boards with the wood and the camera wall mount bracket were connected by long threaded rods. Each NoIR camera were connected to the RasPi, which was placed on the top of the rack, through a camera ribbon cable.

Camera testing, focusing

1. Enabling the NOIR Camera through RasPi Configuration:

The RasPi configuration menu can be reached through typing 'sudo raspi-config' and pressing enter in the Terminal program. Use up and down arrows on the keyboard to travel among different options until hitting 'Interfacing Options' and then press enter. Select 'P1 Camera' and then 'Yes' for the pop-up window. Reboot the RasPi and then test whether the camera works properly by using following command:

$ raspistill –v –o test.jpg

This display will show 5 second preview window and then take a picture and the output image will be saved under your current directory named test.jpg.

2. Trouble shooting of incorrectly working camera:

First, check whether the two ends of the camera cables are connected to either the camera port of RasPi or the port of camera are firmly attached, and whether it is connected to the Camera Port instead of the Display Port on the RasPi.

Second, check whether the camera cable and the camera function properly by switching to other known properly working parts.

Third, run the following command to make sure all software is up to date:

$ sudo apt-get update

$ sudo apt-get upgrade

3. Positioning camera

Run the following command in terminal program on the RasPi:

$ raspistill –t 500

The number represents how many seconds that the preview window will show. It can be changed to any time length that you need.

The field of view, focus, or brightness can be adjusted easily based on the preview window. For this particular research, the distance between the bottom of the camera and the top of the pot is 30cm. The focus can be adjusted by easily twisting the lens. A business card was used for this experiment to make the focusing process easier to judge. To ensure the camera is right above the plant, either move the camera or the plant until the plant appears in the center of the preview window.

This protocol is adapted from an online document. More information can be found here:

https://www.raspberrypi.org/app/uploads/2013/07/RaspiCam-Documentation.pdf

Network multiple Raspberry Pi (RasPi) computers

Eight RasPis were used in this particular experiment, but this protocol can be applied to any quantity of RasPis.

1. Turn on SSH and VNC through RasPi Configuration:

The RasPi configuration menu can be reached through typing ‘sudo raspi-config’ and pressing enter in the Terminal program. Use up and down arrows on the keyboard to travel among different options until hitting ‘Interfacing options’ and then press enter. Scroll down to P2 SSH and press enter. ‘Yes’ will be highlighted, and press enter to turn on SSH. Repeat selecting ‘Interfacing options’, but choose P3 VNC this time and press enter. Use the left arrow to choose ‘Yes’ and press enter, and press ‘OK’ on the next screen.

Press the right arrow twice to select ‘Finish’ which takes you out of the RasPi configuration menu.

2. Change the host name of the RasPis:

Run ‘sudo raspi-config’ again and choose ‘hostname’ as the option. Give it a unique name such as RPi1. Do this for each RasPi on your network so you can easily tell which one you are controlling. Host name can be checked by typing ‘hostname’ and press enter in Terminal program.

3. Setup a local area network (LAN) between RasPi computers:

Connect the RasPis with a powered Ethernet hub through Ethernet cables.

Edit the ‘dhcpcd.conf’ file on RasPi through typing ‘sudo nano /etc/dhcpcd.conf’ and pressing enter in the Terminal program. Use the down arrow on the keyboard to scroll all the way to the end and add the following three lines to the end of the file:

interface eth0

static ip_address=192.168.2.x Note: x can be any unique number from 0 to 254

static routers=192.168.2.254

Press Control-X and then enter to exit nano editor, and press ‘Y’ and then enter to save the changes.

The same changes need to be made on every RasPi on the network except the static ip_address=192.168.2.x must contain a unique number at the end.

Reboot the RasPis. If LAN is set up successfully, connection can be made by typing ‘ssh 192.168.2.x’ (replace ‘x’ with the number you provided) and press enter in Terminal program.

4. Edit ‘interfaces’ file:

Type ‘sudo nano /etc/network/interfaces’ and press enter in the Terminal program. Put a ‘#’ in front of ‘iface eth0 inet dhcp’ to comment it out. Add the following line after it:

iface eth0 inet manual

Press Control-X and then enter to exit nano editor, and press ‘Y’ and then enter to save the changes.

5. Login without using password:

Login to the main RasPi and generate a pair of authentication keys. Type the following command:

$ ssh-keygen –t rsa

Generating public/private rsa key pair.

Enter file in which to save the key: (/home/pi/.ssh/id_rsa):

Press enter for default

Created directory '/home/pi/.ssh'

Enter passphrase (empty for no passphrase):

Press enter for default

Your identification has been saved in /home/pi/.ssh/id_rsa.

Your public key has been saved in /home/pi/.ssh/id_rsa.pub.

Your key fingerprint is:

<a long string of numbers and letters>

Create a directory ~/.ssh as user pi on the remote computer as following:

pi@RPi1: $ ssh pi@RPi2 mkdir –p .ssh

pi@RPi2's password:

Append pi's new public key you generated to pi@RPi2:.ssh/authorized_keys and enter pi's password one last time:

pi@RPi2: $ cat .ssh/id_rsa.pub | ssh pi@RPi1 'cat >> .ssh/authorized_keys'

Using a Virtual Network Connection (VNC) to see the remote RasPi

1. Download the VNC Viewer for RasPi at
   https://www.realvnc.com/download/viewer/raspberrypi/
   Make sure that it says GZ ARM HF in the small window below the SHA number.
2. Transfer the downloaded gzipped file to the RasPi that you want to view the remote RasPis on. In this particular experiment, RPi1 is the main RasPi and VNC was used on this RasPi.

3. After the file has been transferred then unzip the file by double-clicking on it and extracting it.
4. Change the extracted into an executable file by typing 'chmod 755 ~/<path to file>/VNC-Viewer-6.1.1-Linux-ARM' in Terminal program, where <path to file> is the path to the unzipped file (e.g. ~/Desktop/VNC-Viewer-6.1.1-Linux-ARM).
5. Make sure that you have enabled VNC on all the remote RasPi's that you want to view and control (step 1 above). On the remote computer, you will need to enable the screen capture of the VNC server.
6. Double click on the VNC Viewer icon to start VNC Viewer. Choose VNC Viewer under the Pi menu -> Internet -> VNC Viewer
7. Click on the VNC icon and add the IP address for the remote RasPi in the pumped-up window. It should automatically connect and you should be able to see the desktop of the remote RasPi.

Sync clock on multiple RasPis

One feature of RasPi is that the time may be incorrect each time after rebooting the RasPi because it doesn't contain a real-time clock. However, the timing information is usually very important especially for image taking, especially in the later data analysis process. Therefore, it is important to make sure the time is the same on each RasPi on the network to ensure the name of the images were saved correctly. This was done by attaching a Real-Time Clock (RTC) board to the main RasPi I/O pins and setting the main RasPi to be a Network Time Protocol (NTP) server. Each of the eight RasPis with cameras were then set to be NTP clients and all received their time settings from the NTP server on the LAN. This ensures that the time stamp on the files names of each RasPi will be correct.

Transferring images

An USB Flash drive was plugged in to RasPi1 for image storage. On the main RasPi (RasPi1), images were copied by simply using ctrl-C/ctrl-V. For the other RasPis on the LAN the following command was used to help copy images from each RasPi to the USB drive attached to Raspi1:

scp –r pi@192.168.2.x: /home/pi/Desktop/RPix_Images /media/pi/USB_name

LIMITATION OF THE IMAGING STATION SYSTEM

There are some limitations of this imaging system. First, in this particular experiment, due to the image field of view limitation, it only can capture the plant growth stage until the fourth or fifth leaf stage depends on the different growth rates under different light conditions. In the future, the camera could be raised. The mirror could be changed to a larger size in the meantime to obtain a longer period of plant growth.

Second, due to the leaf orientation change through time, some mirrors could not show the exact side view of the plant in some replicates. This might be fixed by adding another mirror at a 90-degree angle.

Notwithstanding these limitations, we have shown how a low-cost imaging method can be used to gain detailed information on plant growth and development under a variety of physiologically relevant conditions, adding to our knowledge of how plants grow.

CHAPTER V

CONCLUSIONS AND FUTURE WORK

CONCLUSIONS

In this thesis, we investigated how *Setaria viridis* responds to different light conditions during growth and development and at flowering time, and how much role the change of light intensity and R:FR ratio plays in different phenotypic responses. One of the main contributions of our work is to open up a new direction of studying the topic of shading by dissecting light intensity and light quality as independent variables, and removing other confounding variables at the same time.

One of our important findings is that the change of light intensity and the change of R:FR ratio showed different degrees of importance for different traits. As a whole, light intensity, light quality and their interaction all played roles in plant responses to shading, which differs from some previous reports. More specifically, the change of light quality had an effect on plant architecture, such as height, number of leaves, and the degree of leaf growth deviation from perfect 180˚ phyllotaxy, while the change of light intensity played a more important role on the traits associated with photosynthesis, such as leaf length, leaf growth rate and the degree of the leaf erectness. We have also found some different results in different growth stages. For example, light intensity had significant effect on height and leaf number at 9 days after germination, but this effect disappeared at flowering time.

The above findings also support the necessity of following growth and development throughout the lifecycle of the plant. Without this data, we would only gain a partial understanding of the roles of light quality and intensity on growth form. Thus, a second contribution of this work is to show how using a low-cost and easy-built imaging station can be used to get large-scale images, and how to use these images to track plant growth and development.

Another important finding is that the responses to shading of *Setaria viridis* differs in several ways from that of other well studied shade avoidance plants. Setaria exhibits increased height, but not earlier flowering or fewer branches, all of which are found in Arabidopsis. These result suggest that Setaria may not be just a shade avoidance plant, but to some extent also showed shade tolerant characteristics

FUTURE WORK

An obvious future direction for this research is to apply directional far-red light to elicit directional plant growth responses. Computational challenges are also still present, as for example in decoupling leaf movement from leaf expansion. Dissecting these two components is a computational challenge for the future.

REFERENCES

Bailey, S., Walters, R. G., Jansson, S., & Horton, P. (2001). Acclimation of *Arabidopsis thaliana* to the light environment: the existence of separate low light and high light responses. Planta, 213(5), 794-801.

Carabelli, M., Sessa, G., Baima, S., Morelli, G., & Ruberti, I. (1993). The *Arabidopsis* Athb-2 and-4 genes are strongly induced by far-red-rich light. The Plant Journal, 4(3), 469-479.

Casal, J., Clough, R., & Vierstra, R. (1996). High-irradiance responses induced by far-red light in grass seedlings of the wild type or overexpressing phytochrome A. Planta, 200(1), 132-137.

Casal, J., Deregibus, V., & Sanchez, R. (1985). Variations in tiller dynamics and morphology in Lolium multiflorum Lam. vegetative and reproductive plants as affected by differences in red/far-red irradiation. Annals of botany, 56(4), 553-559.

Casal, J., Sanchez, R., & Deregibus, V. (1986). The effect of plant density on tillering: the involvement of R/FR ratio and the proportion of radiation intercepted per plant. Environmental and Experimental Botany, 26(4), 365-371.

Casal, J. J. (2012). Shade avoidance. The *Arabidopsis* Book, e0157.

Deregibus, V., Sanchez, R., Casal, J., & Trlica, M. (1985). Tillering responses to enrichment of red light beneath the canopy in a humid natural grassland. Journal of applied Ecology, 199-206.

Deregibus, V. A., Sanchez, R. A., & Casal, J. J. (1983). Effects of light quality on tiller production in Lolium spp. Plant Physiology, 72(3), 900-902.

Devlin, P. F., Halliday, K. J., Harberd, N. P., & Whitelam, G. C. (1996). The rosette habit of Arabidopsis thaliana is dependent upon phytochrome action: novel phytochromes control internode elongation and flowering time. The Plant Journal, 10(6), 1127-1134.

Djakovic‐Petrovic, T., de Wit, M., Voesenek, L. A., & Pierik, R. (2007). DELLA protein function in growth responses to canopy signals. The Plant Journal, 51(1), 117-126.

DIAS-FILHO, M. B. (2000). Growth and biomass allocation of the C4 grasses Brachiaria brizantha and B. humidicola under shade. Pesquisa Agropecuária Brasileira, 35(12), 2335-2341.

Donohue, K., Messiqua, D., Pyle, E. H., Heschel, M. S., & Schmitt, J. (2000). Evidence of adaptive divergence in plasticity: density‐and site‐dependent selection on shade‐avoidance responses in Impatiens capensis. Evolution, 54(6), 1956-1968.

Doust, A. N., Kellogg, E. A., Devos, K. M., & Bennetzen, J. L. (2009). Foxtail millet: a sequence-driven grass model system. Plant Physiology, 149(1), 137-141.

Dubois, P. G., Olsefski, G. T., Flint-Garcia, S., Setter, T. L., Hoekenga, O. A., & Brutnell, T. P. (2010). Physiological and genetic characterization of end-of-day far-red light response in maize seedlings. Plant Physiology, pp. 110.159830.

Easlon, H. M., & Bloom, A. J. (2014). EASY LEAF AREA: AUTOMATED DIGITAL IMAGE ANALYSIS FOR RAPID AND ACCURATE MEASUREMENT OF LEAF AREA. Applications in Plant Sciences, 2(7). doi:10.3732/apps.1400033

Finlayson, S. A., Hays, D. B., & Morgan, P. (2007). phyB-1 sorghum maintains responsiveness to simulated shade, irradiance and red light: far-red light. Plant Cell and Environment, 30(8), 952-962. doi:10.1111/j.1365-3040.2007.01695.x

Franklin, K. A., & Whitelam, G. C. (2005). Phytochromes and shade-avoidance responses in plants. Annals of botany, 96(2), 169-175.

Furbank, R. T., & Tester, M. (2011). Phenomics–technologies to relieve the phenotyping bottleneck. Trends in Plant Science, 16(12), 635-644.

Gehan, M. A., & Kellogg, E. A. (2017). High-throughput phenotyping. American Journal of Botany, 104(4), 505-508.

Gommers, C. M. M., Visser, E. J. W., St Onge, K. R., Voesenek, L., & Pierik, R. (2013). Shade tolerance: when growing tall is not an option. Trends in Plant Science, 18(2), 65-71. doi:10.1016/j.tplants.2012.09.008

Halliday, K. J., Koornneef, M., & Whitelam, G. C. (1994). PHYTOCHROME B AND AT LEAST ONE OTHER PHYTOCHROME MEDIATE THE ACCELERATED FLOWERING RESPONSE OF ARABIDOPSIS-THALIANA L TO LOW RED/FAR-RED RATIO. Plant Physiology, 104(4), 1311-1315.

Johnson, E., Bradley, M., Harberd, N. P., & Whitelam, G. C. (1994). Photoresponses of light-grown phyA mutants of Arabidopsis (phytochrome A is required for the perception of daylength extensions). Plant Physiology, 105(1), 141-149.

Kasperbauer, M. J. (1987). Far-red light reflection from green leaves and effects on phytochrome-mediated assimilate partitioning under field conditions. Plant Physiology, 85(2), 350-354.

Li, L., Ljung, K., Breton, G., Schmitz, R. J., Pruneda-Paz, J., Cowing-Zitron, C., . . . Jung, H.-S. (2012). Linking photoreceptor excitation to changes in plant architecture. Genes & Development, 26(8), 785-790.

Li, P., & Brutnell, T. P. (2011). Setaria viridis and Setaria italica, model genetic systems for the Panicoid grasses. Journal of Experimental Botany, 62(9), 3031-3037.

Maddonni, G. A., Otegui, M. a. E., Andrieu, B., Chelle, M., & Casal, J. J. (2002). Maize leaves turn away from neighbors. Plant Physiology, 130(3), 1181-1189.

Mathews, S. (2006). Phytochrome ‐ mediated development in land plants: red light sensing evolves to meet the challenges of changing light environments. Molecular Ecology, 15(12), 3483-3503.

Mathews, S., & Sharrock, R. (1997). Phytochrome gene diversity. Plant, Cell & Environment, 20(6), 666-671.

Milenkovic, L., Ilic, Z. S., Durovka, M., Kapoulas, N., Mirecki, N., Fallik, E. (2012). Yield and pepper quality as affected by light intensity using colour shade nets. Agricultural & Forestry, 58(1), 19-33.

Millenaar, F. F., Cox, M. C., van Berkel, Y. E. d. J., Welschen, R. A., Pierik, R., Voesenek, L. A., & Peeters, A. J. (2005). Ethylene-induced differential growth of petioles in Arabidopsis. Analyzing natural variation, response kinetics, and regulation. Plant Physiology, 137(3), 998-1008.

Mitchell, K. (1953). Influence of light and temperature on the growth of ryegrass (Lolium spp.) I. Pattern of vegetative development. Physiologia plantarum, 6(1), 21-46.

Morgan, D., & Smith, H. (1978). The relationship between phytochrome-photoequilibrium and Development in light grown Chenopodium album L. Planta, 142(2), 187-193.

Morgan, D. C., & Smith, H. (1976). Linear relationship between phytochrome photoequilibrium and growth in plants under simulated natural radiation. Nature, 262(5565), 210-212.

Mullen, J. L., Weinig, C., & Hangarter, R. P. (2006). Shade avoidance and the regulation of leaf inclination in Arabidopsis. Plant, Cell & Environment, 29(6), 1099-1106.

Mutka, A. M., & Bart, R. S. (2014). Image-based phenotyping of plant disease symptoms. Frontiers in plant science, 5.

Ni, M., Tepperman, J. M., & Quail, P. H. (1998). PIF3, a phytochrome-interacting factor necessary for normal photoinduced signal transduction, is a novel basic helix-loop-helix protein. Cell, 95(5), 657-667.

Ni, M., Tepperman, J. M., & Quail, P. H. (1999). Binding of phytochrome B to its nuclear signalling partner PIF3 is reversibly induced by light. Nature, 400(6746), 781.

Pedmale, U. V., Celaya, R. B., & Liscum, E. (2010). Phototropism: mechanism and outcomes. The Arabidopsis Book, e0125.

Quail, P. H. (1994). Phytochrome genes and their expression Photomorphogenesis in plants (pp. 71-104): Springer.

Reed, J. W., Nagpal, P., Poole, D. S., Furuya, M., & Chory, J. (1993). Mutations in the gene for the red/far-red light receptor phytochrome B alter cell elongation and physiological responses throughout Arabidopsis development. The Plant Cell, 5(2), 147-157.

Rominger, J. M. (1962). Taxonomy of Setaria (Gramineae) in North America. 29. Illinois biological monographs; v. 29.

Sasidharan, R., Chinnappa, C., Staal, M., Elzenga, J. T. M., Yokoyama, R., Nishitani, K., . . . Pierik, R. (2010). Light quality-mediated petiole elongation in Arabidopsis during shade avoidance involves cell wall modification by XTHs. Plant Physiology, pp. 110.162057.

Sadava, D. E., Hillis, D. M., Heller, H. C., & Berenbaum, M. (2014). Life: The science of biology. Sunderland, MA: Sinauer.

Schmitt, J. (1997). Is photomorphogenic shade avoidance adaptive? Perspectives from population biology. Plant, Cell & Environment, 20(6), 826-830.

Schmitt, J., Stinchcombe, J. R., Heschel, M. S., & Huber, H. (2003). The adaptive evolution of plasticity: phytochrome-mediated shade avoidance responses. Integrative and Comparative Biology, 43(3), 459-469.

Sellaro, R., Crepy, M., Trupkin, S. A., Karayekov, E., Buchovsky, A. S., Rossi, C., & Casal, J. J. (2010). Cryptochrome as a sensor of the blue/green ratio of natural radiation in Arabidopsis. Plant Physiology, pp. 110.160820.

Smith, H. (1982). Light quality, photoperception, and plant strategy. Annual review of plant physiology, 33(1), 481-518.

Smith, H. (1995). Physiological and ecological function within the phytochrome family. Annual review of plant biology, 46(1), 289-315.

Smith, H., & Holmes, M. (1977). The function of phytochrome in the natural environment—III. Measurement and calculation of phytochrome photoequilibria. Photochemistry and Photobiology, 25(6), 547-550.

Smith, H., & Whitelam, G. C. (1997). The shade avoidance syndrome: Multiple responses mediated by multiple phytochromes. Plant Cell and Environment, 20(6), 840-844. doi:10.1046/j.1365-3040.1997.d01-104.x

Smith, H., Xu, Y., & Quail, P. H. (1997). Antagonistic but complementary actions of phytochromes A and B allow optimum seedling de-etiolation. Plant Physiology, 114(2), 637-641.

Sysoeva, M. I., Markovskaya, E. F., & Shibaeva, T. G. (2010). Plants under continuous light: a review. Plant stress, 4(1), 5-17.

Xianmin DIAO, J. S., Jeffrey L. BENNETZEN,Jiayang LI. (2014). Initiation of Setaria as a model plant. Front. Agr. Sci. Eng., 1(1), 16-20. doi:10.15302/j-fase-2014011

Yokawa, K., & Baluška, F. (2018). Sense of space: Tactile sense for exploratory behavior of roots. Communicative & integrative biology, 11(2), 1-5.

Yoshida, S., Navasero, S., & Ramirez, E. (1969). Effects of silica and nitrogen supply on some leaf characters of the rice plant. Plant and soil, 31(1), 48-56.

APPENDICES

APPENDIX A: Images of experimental setup with labels.

A) Overall view. B) Close view of the plant growing environment. C) Top view of the plant with a side view in the mirror. D) Close view of the light sources with Raspberry Pi cameras and Infrared lights.

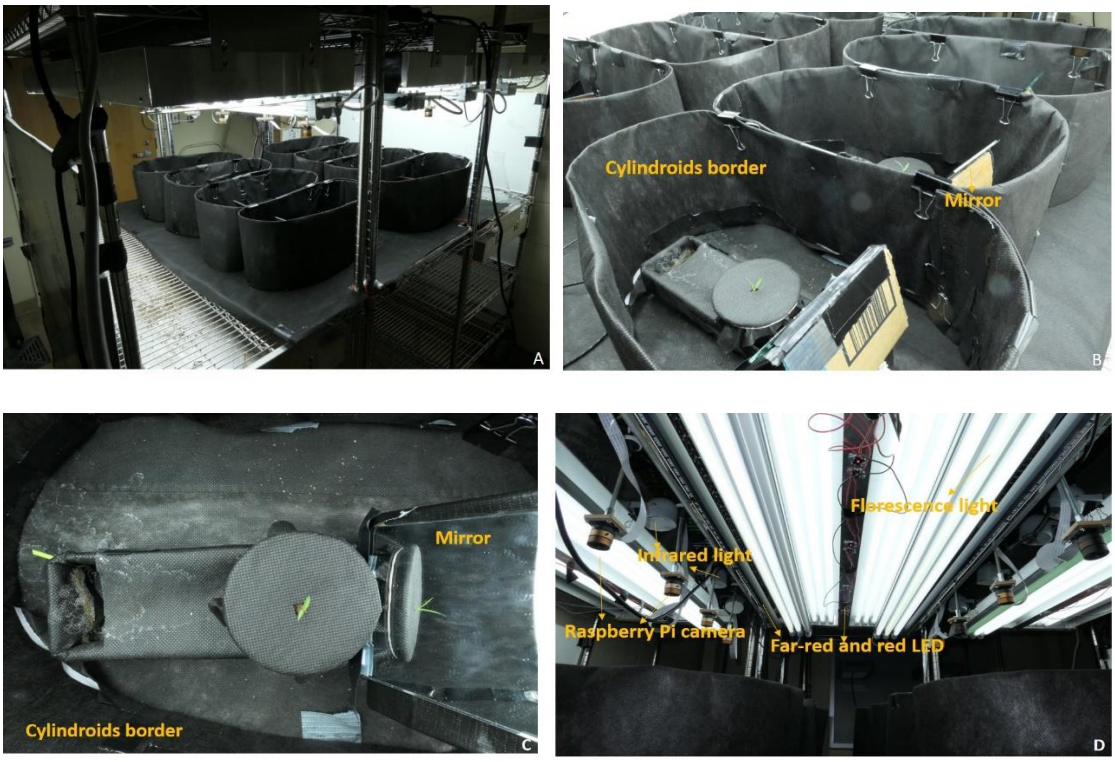

APPENDIX B: Two-way ANOVA for eight phenotypic measurements at flowering time.

Days to Flower	DF	Sum of Squares	Mean Square	F-value	P-value	Partial Eta Squared
Light intensity	1	76.6	76.56	11.78	0.0011**	0.16
Light quality	1	39.1	39.06	6.01	0.017*	0.091
Light intensity × light quality	1	6.2	6.25	0.961	0.33	0.016
Residuals	60	390.1	6.5			

Number of Leaves	DF	Sum of Squares	Mean Square	F-value	P-value	Partial Eta Squared
Light intensity	1	1.89	1.89	1.30	0.26	0.021
Light quality	1	62.02	62.02	42.68	1.56E-08***	0.42
Light intensity × light quality	1	21.39	21.39	14.72	0.00030***	0.20
Residuals	60	87.19	1.45			

Height	DF	Sum of Squares	Mean Square	F-value	P-value	Partial Eta Squared
Light intensity	1	6.5	6.5	0.33	0.57	0.0054
Light quality	1	1421.3	1421.3	71.62	8.00E-12***	0.54
Light intensity × light quality	1	261.6	261.6	13.18	0.00059***	0.18
Residuals	60	1190.8	19.8			

Number of Tillers	DF	Sum of Squares	Mean Square	F-value	P-value	Partial Eta Squared
Light intensity	1	0.14	0.14	0.62	0.44	0.010
Light quality	1	0.14	0.14	0.62	0.44	0.010
Light intensity × light quality	1	4.52	4.52	19.80	3.80E-05***	0.25
Residuals	60	13.69	0.23			

Leaf Length	DF	Sum of Squares	Mean Square	F-value	P-value	Partial Eta Squared
Light intensity	1	283.1	283.08	30.71	7.05E-07***	0.34
Light quality	1	31.9	31.92	3.46	0.068	0.055
Light intensity × light quality	1	93.6	93.61	10.16	0.0023**	0.14
Residuals	60	553	9.22			

Leaf Width	DF	Sum of Squares	Mean Square	*F*-value	*P*-value	Partial Eta Squared
Light intensity	1	0.49	0.49	16.92	0.00012***	0.22
Light quality	1	0.72	0.72	24.95	5.39E-06***	0.29
Light intensity × light quality	1	1	1	34.53	1.97E-07***	0.37
Residuals	60	1.74	0.029			

Inflorescence Length	DF	Sum of Squares	Mean Square	F-value	P-value	Partial Eta Squared
Light intensity	1	0.83	0.83	2.72	0.11	0.043
Light quality	1	27.43	27.43	89.47	1.68E-13**	0.60
Light intensity × light quality	1	25.63	25.63	83.59	5.68E-13**	0.58
Residuals	60	18.40	0.31			

Dry Biomass	DF	Sum of Squares	Mean Square	F-value	P-value	Partial Eta Squared
Light intensity	1	0.66	0.66	99.01	2.58E-14***	0.62
Light quality	1	1.37	1.37	205.08	2.00E-16***	0.77
Light intensity × light quality	1	0.98	0.98	146.31	2.00E-16***	0.71
Residuals	60	0.40	0.0067			

APPENDIX C: Two-way ANOVA for height, length of internode 1 and number of leaves at 9 DAG.

Height	DF	Sum of Squares	Mean Square	*F*-value	*P*-value	Partial Eta Squared
Light intensity	1	5400	5400	18.58	6.79E-05***	0.28
Light quality	1	12049	12049	41.46	3.12E-08***	0.43
Light intensity × light quality	1	5677	5677	19.53	4.69E-05***	0.26
Residuals	55	15983	291			

Distance between successive leaves	DF	Sum of Squares	Mean Square	*F*-value	*P*-value	Partial Eta Squared
Light intensity	1	1761	1760.8	16.068	0.00019***	0.24
Light quality	1	1273	1272.6	11.613	0.0012**	0.17
Light intensity × light quality	1	747	746.8	6.815	0.012*	0.11
Residuals	55	6027	109.6			

Number of leaves	DF	Sum of Squares	Mean Square	*F*-value	*P*-value	Partial Eta Squared
Light intensity	1	4.74	4.74	19.73	4.35E-05***	0.24
Light quality	1	8.13	8.13	33.87	3.14E-07*	0.38
Light intensity × light quality	1	0.040	0.040	0.17	0.69	0.0030
Residuals	55	13.20	0.24			

Third leaf length	DF	Sum of Squares	Mean Square	*F*-value	*P*-value	Partial Eta Squared
Light intensity	1	41513	41513	25.54	5.11E-06***	0.31
Light quality	1	1449	1449	0.89	0.35	0.016
Light intensity × light quality	1	296	296	0.18	0.67	0.0033
Residuals	55	89385	1625			

Third leaf growth rate	DF	Sum of Squares	Mean Square	*F*-value	*P*-value	Partial Eta Squared
Light intensity	1	4.29	4.29	11.42	0.0013**	0.16
Light quality	1	0.013	0.013	0.034	0.85	0.00057
Light intensity × light quality	1	0.23	0.23	0.603	0.44	0.0099
Residuals	60	22.56	0.38			

Δz	DF	Sum of Squares	Mean Square	*F*-value	*P*-value	Partial Eta Squared
Light intensity	1	7897	7897	26.12	5.53E-06***	0.35
Light quality	1	20	20	0.065	0.80	0.0014
Light intensity × light quality	1	449	449	1.49	0.23	0.030
Residuals	48	14514	302			

Rectangle width	DF	Sum of Squares	Mean Square	*F*-value	*P*-value	Partial Eta Squared
Light intensity	1	9429	9429	8.23	0.0058**	0.12
Light quality	1	28060	28060	24.48	6.8E-06***	0.30
Light intensity × light quality	1	8224	8224	7.17	0.0096**	0.11
Residuals	58	66494	1146			

VITA

Qing Li

Candidate for the Degree of

Master of Science

Thesis: GROWTH AND DEVELOPMENT OF *SETARIA VIRIDIS* (POACEAE) UNDER NORMAL AND SHADED LIGHT REGIMES

Major Field: Plant Biology

Biographical:

Education:

Completed the requirements for the Master of Science in Plant Biology at Oklahoma State University, Stillwater, Oklahoma in December, May, 2019.

Completed the requirements for the Bachelor of Science in Biology at Doane University, Crete, Nebraska in 2016.

Professional Memberships:
Botanical Society of America